6 Glenoid Anatomy and Biomechanics

Michael Codsi

Normal Glenoid Anatomy

The glenoid anatomy has classically been defined by the articular surface anatomy. The height and width of the glenoid have been measured in anthropomorphic studies, and each study has used a slightly different methodology to measure the glenoid. Mallon et al. evaluated 28 cadaver scapulae and measured the height and width in both men and women [65]. They found the average height of the glenoid was 38 mm (range, 33–45) for men and was 36.2 mm (range, 32–43) for women. Iannotti et al. measured the height of the glenoid in 140 cadaver scapulae and found the average height was 39 mm (range, 30–48 mm) and the average glenoid width was 29 mm (range, 21–35 mm) [49]. He also reported the distribution of the sizes of the glenoid and separated them into five groups according to their height and four groups according to their width. Churchill et al. measured the height and width of the glenoid using 344 cadaver scapulae from the Hamann-Todd Osteological Collection, the Museum of Natural History in Cleveland, Ohio [19]. They used scapulae from persons who were between 20 and 30 years old at the time of death. The average glenoid height in men was 37.5 mm (range, 30–43 mm), and the average width was 27.8 mm (range, 24–33 mm). For women, the average height was 32.6 mm (range, 29–37 mm), and the average width was 23.6 mm (range, 20–26 mm). Checroun et al. measured the glenoid dimensions in 412 cadaver scapulae and found an average height of 37.9 mm (range, 31–50 mm) [17]. The average width of the glenoids was 29.3 mm (range, 23–42 mm). Kwon et al. measured the height and width of the glenoid in 12 cadaver specimens using both manual measurements and CT scan measurements to determine the accuracy of CT scan measurements and found that the difference in measurements was within 2 mm [60]. The median glenoid height was 37.8 mm (range, 30–47 mm), and the median width was 26.8 mm (range, 22–35 mm) when the measurements from the specimens were used (Table 6.1).

Glenoid Version

Glenoid version has been measured in multiple studies, and the methodology used to measure the version is an important variable to understand, because two different methods can give different version measurements for the same scapula. It is also difficult to obtain radiographs with excellent technique because the patient with severe arthritis often has difficulty moving the shoulder in the

M. Codsi, MD
Department of Evergreen Orthopedic Sports Care, Evergreen Hospital, 12333 NE 130th Lane Suite 410, Kirkland, WA 98034, USA
e-mail: mjcodsi@evergreenhealth.com

© Springer International Publishing Switzerland 2016
A.D. Armstrong, A.M. Murthi (eds.), *Anatomic Shoulder Arthroplasty*,
DOI 10.1007/978-3-319-29164-2_6

Table 6.1 Glenoid height and width measurements

Author	Year	Specimens	Glenoid height	Glenoid width
Mallon et al.	1992	28	38 mm (range, 33–45 mm)	
Iannotti et al.	1992	140	39 mm (range, 30–48 mm)	29 mm (range, 21–35 mm)
Churchill et al.	2001	344	37.5 mm (range, 30–43 mm)	23.6 mm (range, 20–26 mm)
Checroun et al.	2002	412	37.9 mm (range, 31–50 mm)	29.3 mm (range, 23–42 mm)
Kwon et al.	2005	12	37.8 mm (range, 30–47 mm)	26.8 mm (range, 22–35 mm)

positions needed to get the best views of the glenoid. Surprisingly, radiographs are often easier to obtain after total shoulder arthroplasty because the patient's range of motion is better and the landmarks on the radiograph are easier to measure because the joint space has been restored with the prosthetic implants. Glenoid version has been traditionally measured using standard radiographs, but the accuracy of this method was questioned in a study done by Nyffeler et al. [73]. They measured glenoid version in 25 patients without arthritis and 25 patients after total shoulder arthroplasty using radiographs and CT scans. They found that glenoid retroversion was overestimated with radiographs 86 % of the cases and the difference between the CT scan and radiographic measurement was 6.5° (range, 0–21°). The correlation between the CT measurements and the radiographs was higher (0.67) in the total shoulder group compared to the instability group (0.33). Based on these results, the authors recommended the use of CT scan as the preferred modality to measure postoperative glenoid version in total shoulder arthroplasty. A similar study was done by Ho et al. to evaluate the accuracy of radiographs compared to CT scans for the measurement of glenoid version in cases before and after total shoulder arthroplasty [43]. Thirty-two patients had radiographs and CT scans taken before and after surgery, and multiple measurements were made including glenoid version. There was moderate agreement between CT scan and radiographic measurements (0.69) and the radiographs overestimated glenoid version by 4.2°.

As the use of standard two-dimensional CT scans has increased for the measurement of glenoid version, other methods have emerged with the advent of three-dimensional CT software. This software allows for the measurements of glenoid version to be done on the same scapula with different methods. Bryce et al. described this variation in an elegant study using 40 scapulae CT scans [10]. The scans were imported into a software program called MATLAB that allowed for manipulation of the scapula orientation and calculation of the resulting glenoid version. It helps to understand the variation in measurement by starting with the classic method of measuring glenoid version. First, a plane of the scapula must be defined from which the version of the glenoid articular surface can be measured against. The plane of the scapula is typically defined by three points on the scapula, the center of the glenoid, the tip of the inferior scapular angle, and a point at the intersection of the spine of the scapula with the medial border of the scapula (Fig. 6.1). Second, the plane of the glenoid articular surface is defined. This can be done using two points on the anterior and posterior edges of the glenoid surface halfway between the superior and inferior pole of the glenoid. It can also be done using three points anywhere around the edge of the glenoid articular surface. Third, the version measurement can then be made using the angle formed by the two planes. This seems easy to do when using a three-dimensional model or when measuring the version with a real scapula. The variation in the measurement occurs when the scapula is shown using two-dimensional images. If the two-dimensional images are rendered with the scapula rotated in abduction or adduction, then the plane of the glenoid articular surface changes and so does the version. The variation in the version measurements can be quite substantial and can range from 4.7° of anteversion to 10.6° of retroversion on the same scapula depending on the orientation of the scapula. Regression analysis for scapula rotation in the coronal plane showed that

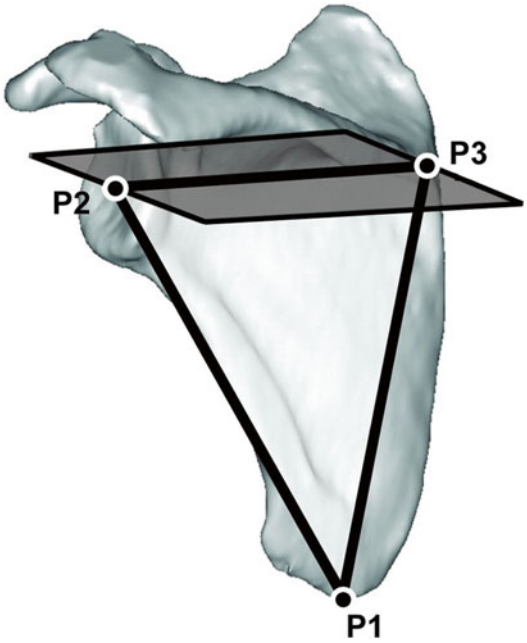

Fig. 6.1 The plane of the scapula is defined by the most distal point of the inferior scapular angle (*P1*), the center of the glenoid fossa (*P2*), and the point at the vertebral border where the scapular spine intersects the medial border of the scapular (*P3*) (Reprinted with permission from Bryce et al. [10])

Table 6.2 Glenoid version measurements

Author	Year	Specimens	Glenoid version
Cyprien et al.	1983	50	8 degrees of retroversion
Friedman et al.	1992	62	2 degrees of anteversion
Mallon et al.	1992	28	6 degrees of retroversion
Couteau et al.	2001	28	8 degrees of retroversion
Churchill et al.	2001	344	1 degrees of retroversion
Scalise et al.	2008	14	7 degrees of retroversion
Ganapathi et al.	2011	19	7 degrees of retroversion
Matsumura et al.	2012	410	1 degree of retroversion

every one degree of scapular abduction led to 0.42° of version variability and every one degree of scapular adduction resulted in 0.16° of version variability. The effect of abduction on version variability was significantly stronger than the effect of adduction on version variability. At 20° of scapular abduction, the mean version variation was 9.4°, and for 20° of adduction, the mean version variation was 2.4°. These findings were confirmed in another follow-up study by the same group [13] (Table 6.2).

Cyprien et al. measured the version of the glenoid using x-rays from 50 normal patients and 15 patients who had recurrent anterior dislocations [25]. They found the average normal version was 7.1° for retroversion compared to 8.9° for retroversion in the patients with recurrent dislocations. Friedman et al. used two-dimensional CT scans of 63 normal patients and compared them to a group of 20 patients with glenohumeral arthritis [31]. The average anteversion of the normal group was 2° (range, +14 to −12°), and the average retroversion of the arthritis group was 11° (range, +2 to −32°). Mallon et al. evaluated the version in 28 cadaver scapulae and found the average retroversion was 6° (range, +2 to −13°) [65]. Couteau et al. measured the version of 28 scapula using two-dimensional CT scan measurements [24]. The patients included in the study had rotator cuff tears without glenohumeral arthritis, glenohumeral arthritis, and rheumatoid arthritis. The average retroversion of the group of patients with rotator cuff tears was 8° (range, 2–17°), with glenohumeral arthritis 16° (range, 0–50°), and the patients with rheumatoid arthritis have an average retroversion of 15° (range, 6–22°).

Churchill et al. measured the version of 344 scapulae from the Hamann-Todd Osteological Collection at the Museum of Natural History, in Cleveland, Ohio [19]. This collection contains skeletons of Cleveland's unclaimed dead from 1912 through 1938. The ages of the specimens were between 20 and 30 years. They measured the version using two different points to define the plane of the scapula. One measurement used the junction of the spine of the scapula with the medial border of the scapula, and the other measurement used a point closer to the superior medial angle of the scapula (Fig. 6.2). The average version using the junction of the spine of the scapula and the medial border of the scapula was 1.23° (range, −10 to +10°). There was no difference when

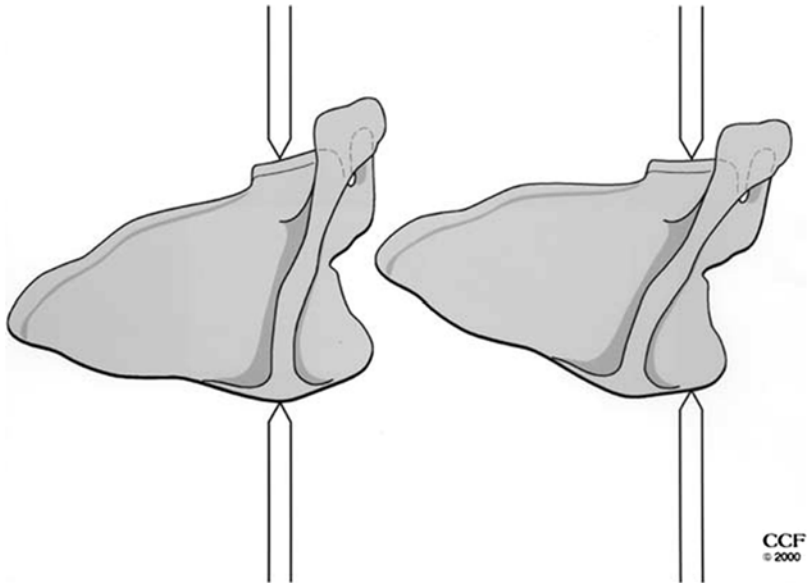

Fig. 6.2 Comparison of the two different scapular positions studied. *Left*, The transverse axis of the scapula is identified by the platform pins. *Right*, The scapula has been rotated such that the glenoid inclination is parallel to the base plate. Note that the moving platform pin maintains the same position as before, but the base platform pin no longer is positioned along the scapular spine (Reprinted from Churchill et al. [19] with permission from Elsevier)

comparing the men and women in the group. When using the alternative point on the superior medial angle of the scapula, the average version was not statistically different.

Matsumura et al. performed a more recent study in a population of healthy Japanese volunteers and found a wide range of glenoid version measurements [66]. The average glenoid retroversion was 1° with a range from 9° of anteversion to 13° of retroversion. Glenoid retroversion was higher on the dominant side in all patients, and it was higher in men compared to women.

Scalise et al. measured the version of 14 patients with osteoarthritis in one shoulder and measured the version of the opposite normal shoulder using a three-dimensional CT [87]. A custom software program was used to define the plane of the scapula so the measurements would match the technique described by Churchill et al. in their study. The average retroversion of the normal shoulders was 7° (range, 0–14°), and the average retroversion for the arthritic side was 15.6° (range, −1–33°).

Ganapathi et al. measured the version of 58 normal scapulae from the Hamann-Todd Collection using three-dimensional CT scan renderings [33]. They compared the normal cadaver scapulae to humans who had osteoarthritis in one shoulder and their normal non-arthritic shoulders. The humans with normal bilateral shoulders had an average version of 2.59°. The average retroversion of the glenoids on the normal side of the matched pairs was 6.8°, and the average retroversion of the arthritic matched pair of glenoids was 14.7°. This data suggests, but does not prove, that patients with a retroverted glenoid are more likely to develop osteoarthritis of the shoulder. It may also suggest that the normal version for patients with osteoarthritis is different from the normal version of patients without osteoarthritis. This has important implications for surgeons who must decide how much version should be corrected when performing a total shoulder replacement with a glenoid implant.

Hendel et al. studied the effect of using patient-specific instruments to position the glenoid component during anatomic total shoulder replacement surgery [41]. They used three-dimensional CT scans for 34 patients with osteoarthritis and found the average retroversion for the glenoid was 14.3° (range, +7–27°). The importance of all of these

studies, which report their measurements of glenoid version, is that there is a wide range of version measurements to take into consideration. The range of version measurements can be due to differences in the techniques used to measure the version based on the rotation of the scapula and the tilt of the scapula. Many of the studies, however, used three-dimensional renderings of the CT scans, which correct for any variation in the techniques used to obtain the CT scan data. A few of the studies used the same patient population, namely, the Hamann-Todd Osteological Collection, which may not be generalizable to the general population.

Glenoid Vault

While a lot of study has focused on describing the anatomy of the glenoid articular surface, relatively few studies in the past have described the anatomy of the glenoid walls and the bone beneath the articular surface. This anatomy has become more important to understand as surgeons start to deal with bone deformity and bone loss due to severe disease and to failure of shoulder replacements. In complex cases, glenoid implants require fixation points beyond the articular surface, and with the advent of the reverse total shoulder, the glenoid component relies on fixation points in the glenoid vault and further medial into the body of the scapula. Investigations into the unique shape of the glenoid vault have also led to a better understanding of glenoid version and its relationship to glenohumeral arthritis.

Bicknell et al. measured the endosteal dimensions of the glenoid vault in 72 scapulae with a mean age of 70 years [7]. The dimensions were larger for males compared to females, but there was no relationship between the dimensions and age or between the presence and absence of arthritis. The shape of the endosteal dimensions was relatively consistent, and there was a small distribution of sizes. The shape of the glenoid vault is relatively straight-sided, or rectangular, in the coronal plane and more highly fluted, or triangular, in the transverse plane.

Codsi et al. selected 61 cadaver scapulae from the Hamann-Todd Osteological Collection to study the shape of the glenoid vault [21]. A wide range of sizes were selected in order to define the normal glenoid vault anatomy. CT scans of each scapula were performed, and the data were analyzed using a custom software program to measure and manipulate the images. The two-dimensional slices of the glenoid vault in the axial plane were used to trace the inner surface area of the glenoid vault (Fig. 6.3). The points on the tracings were recorded, and then the points from each CT slice were stacked on top of one another to create a three-dimensional shape of each vault (Figs. 6.4, 6.5, and 6.6). The vaults were then standardized to one size based on the height of the glenoid articular surface, which allowed for comparison of the shape of the glenoid vault among the different sized scapulae. The right-sided vaults were mirrored about the XZ plane so they could be compared to the left-sided vaults. Two vaults were overlapped, and the distance between the closest tracing points on each vault was measured. The average distance between 85 % of all the tracing points was less than 2 mm from each other, indicating that the shapes of the glenoid vaults in this study were relatively uniform. The shape of the standardized glenoid vault was then made into a plastic model along with four other sizes that were 10 % and 20 % larger and smaller to correspond with the sizing characteristics for a traditional anatomic glenoid implant. These plastic models were then implanted into cadaver scapulae that were not included in the original 61 scapulae used to generate the shape of the models. The cadavers with the plastic models were then scanned with a CT scanner, and the distances between the models and the endosteal bone of the cadaver glenoid vaults were measured. The average distance between the plastic models and endosteal bone was 2.4 mm, and 80 % of the points measured were within 3 mm.

When confronted with a deformity of the glenoid, the surgeon needs to decide how much of the deformity to correct when implanting a glenoid component. Based on the anatomic studies, there is a wide range of normal glenoid version, so it can be difficult to determine what the patient's normal glenoid anatomy was like before the pathology became severe and deformed the glenoid. Scalise et al. wanted to use the shape of

the glenoid vault to find out if there was a way to predict what the vault and the articular surface looked like before the pathology deformed the glenoid [87]. Fourteen patients had CT scans of the arthritic shoulder and the normal opposite shoulder. Using a custom three-dimensional software program, the shape of the glenoid vault was place inside the pathologic glenoid, and the version of the glenoid vault shape was measured. Then at a separate sitting, the glenoid vault shape was placed into the glenoids of the normal shoulders and the version of the glenoid vault shape was measured. The version of the glenoid vault was the same for the arthritic shoulders and the normal shoulder for each patient. These data suggest that the version of the native arthritic glenoid can be predicted using the glenoid vault shape (Fig. 6.7). This may be helpful for surgeons to know when they are deciding how much correction of retroversion should be done during placement of the glenoid component.

Fig. 6.4 Three-dimensional left glenoid vault model showing the articular surface and the anterior wall of the glenoid vault

Scapula Anatomy

With the advent of the reverse total shoulder replacement that uses a glenoid implant fixed to the scapula with screws, more research was done to understand the anatomy of the scapula medial to

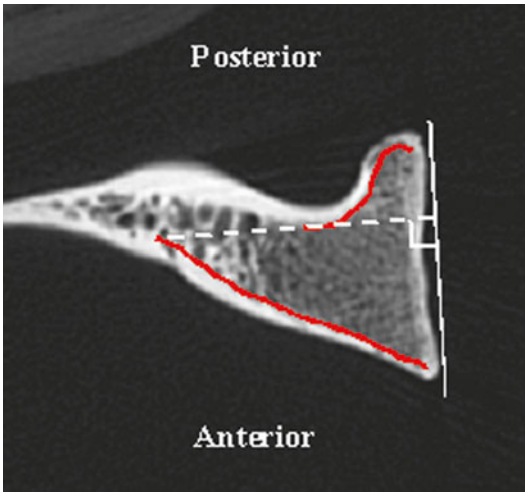

Fig. 6.3 This axial CT scan image shows the inner endosteal walls of the glenoid vault (Reprinted from Codsi et al. [21] with permission from Elsevier)

Fig. 6.5 Three-dimensional left glenoid vault model showing the medial ridge of the vault. The articular surface is facing away from the drawing (not seen). The posterior wall is to the left of the photo, and the anterior wall is on the right side of the photo

the glenoid surface and the glenoid vault. Codsi et al. used three-dimensional CT scans to determine the best locations to place screws from the

glenoid articular surface to the body of the scapula [22]. Twenty-seven scapulae were scanned into a custom software program that allowed the manipulation of the scapula to virtually implant screws of different lengths into the bone. Three locations in the scapula body were found that could accommodate long screws. The first was the superior screw, which started in the superior portion of the glenoid and was directed toward the base of the coracoid. The second screw started in the middle of the glenoid and went through the middle of the scapula (Fig. 6.8a–c). The third screw location started on the inferior glenoid surface and was directed along the lateral cortical border of the scapula. The length of the screws could be as long as 75 mm if placed perfectly, but any deviation in the angle of the insertion by 15° would alter the length of the screws between 17 and 30 mm. When the constraint of an implant was introduced, the lengths of the screws were much shorter as well. Using the current implant designs that feature a central screw or fixation, this screw can be placed in the location described as the central screw in this study. The other superior and inferior screw locations are not typically useful with the current implants available because they do not allow for the high angle of insertion needed to place the screw in those positions of the scapula.

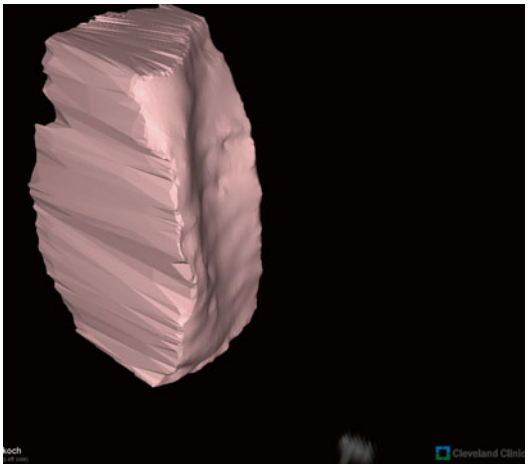

Fig. 6.6 Three-dimensional left glenoid vault model showing the articular surface and the posterior wall of the vault

Humphrey et al. studied the anatomy of the ten cadaver scapulae to find the best locations for screw placement to secure metal glenoid implants [48]. They described three columns of bone in the scapula body that could be used for screw placement, which were similar to the ones described previously. These include the base of the coracoid, the scapula spine, and the scapula pillar. They implanted a glenoid baseplate for a reverse total shoulder into the scapula and measured the

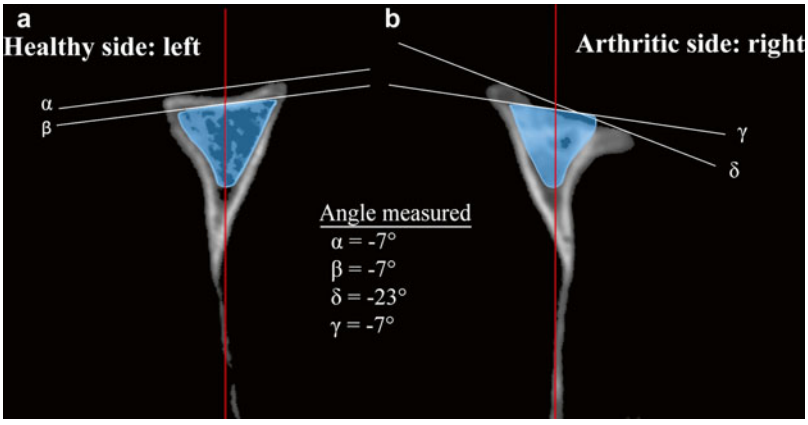

Fig. 6.7 Example of glenoid version measurements after vault model placement in both scapulae of a subject with unilateral osteoarthritis. The plane of the scapula is represented by the red line. (**a**) On the healthy side, the glenoid version measures -7 degrees (*α line*), and the vault model also measures -7 degrees (*β line*). (**b**) On the arthritic side, the glenoid version measures -23 degrees (*δ line*). However, in the arthritic glenoid, the vault model measures -7degrees, (*γ line*) just as measured on the healthy, contralateral side (Reprinted from Scalise et al. [87] with permission from Elsevier)

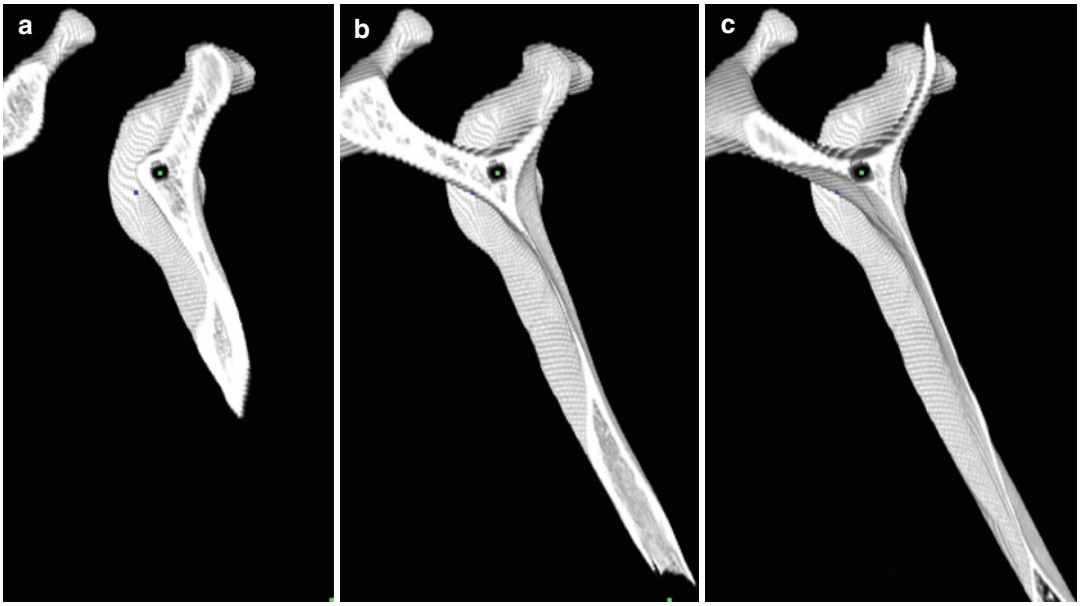

Fig. 6.8 Cross-sectional CT scan images of a scapula with a central screw hole starting at the center of the glenoid articular surface and exiting at the junction of the scapula spine and medial border of the scapula (Reprinted from Codsi et al. [22] with permission from Elsevier). (**a**) Cross section of the scapula 2 cm medial to the glenoid surface, (**b**) Cross section in the middle of the scapula, (**c**) Cross section 2 cm from the medial border of the scapula

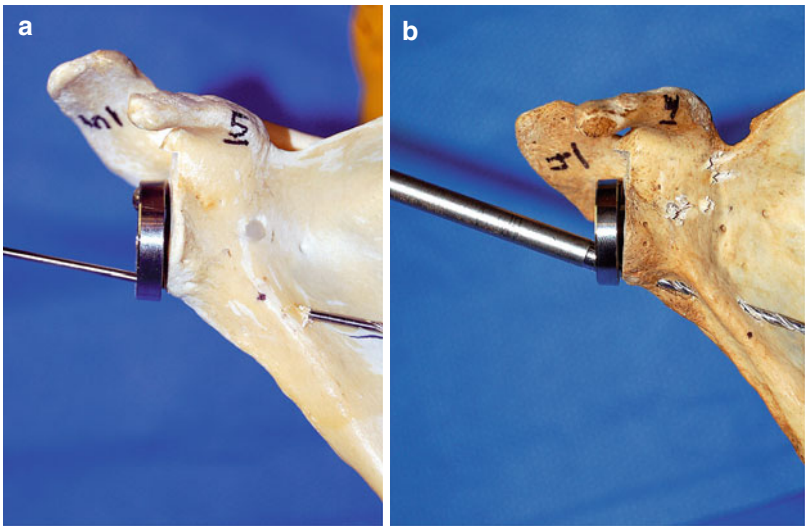

Fig. 6.9 (**a**) The drill bit stays completely within the bone before exiting the cortex medially. (**b**) An "in-out-in" configuration. The drill bit comes out of bone and then goes back into bone before engaging the medial cortex (Reprinted from Humphrey et al. [48] with permission from Elsevier)

length of the screws that could be placed. The average superior screw length was 36 mm (range, 29–40 mm) and the inferior screw was 47 mm (range, 45–54 mm). The authors also noted that the use of a variable angle screw allowed for longer screws because the superior screw could be angled toward the base of the coracoid and the inferior screw could be angled toward the scapular pillar. These two locations are not 180° from each other, so a fixed angle baseplate would only allow perfect placement into one of these locations (Figs. 6.9, 6.10, and 6.11).

Fig. 6.10 The three-column concept. (**a**) Each column consists of bone that is suitable for achieving strong screw purchase. The columns are the base of the coracoid (*1*), the spine of the scapula (*2*), and the scapular pillar (*3*). (**b**) The paucity of bone between the columns becomes evident when the scapula is transilluminated. (**c**) An exploded view of the scapula demonstrates the columns. The thick bone can be seen at the cross sections of the scapular spine and the pillar (*white arrows*). The bone in between the columns is often paper thin (Reprinted from Humphrey et al. [48] with permission from Elsevier)

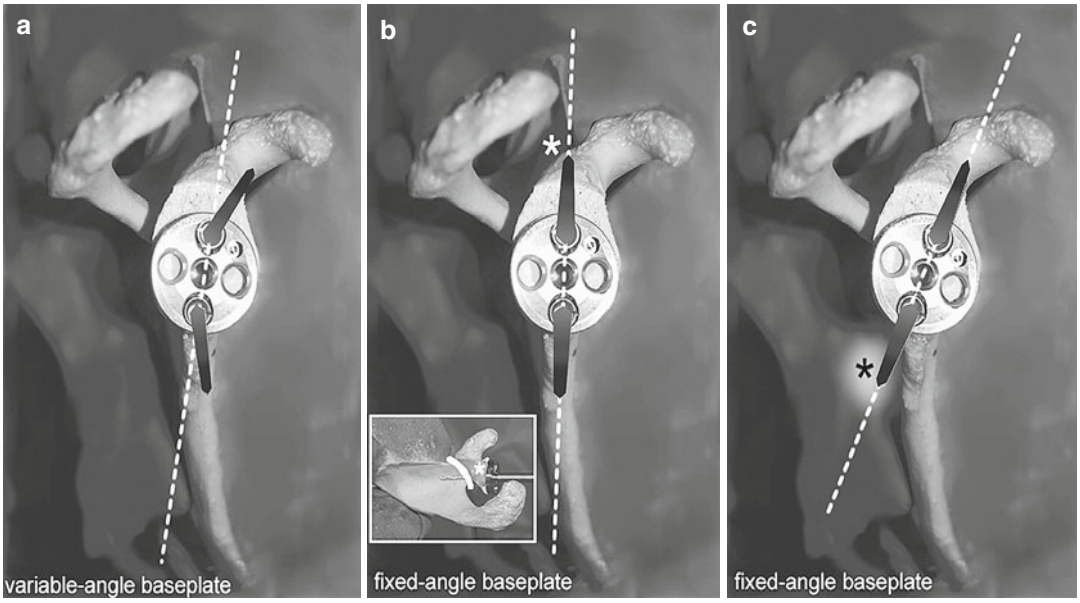

Fig. 6.11 The effect of baseplate rotation on superior and inferior screw trajectory. (**a**) The variable angle baseplate allows the surgeon to direct the screws to the appropriate bony columns. (**b**) With a fixed-angle baseplate, rotating the component so that the inferior screw captures the pillar will lead to penetration of the superior screw outside of the scapular "safe zone" (*white asterisk*). The subwindow shows a drill bit violating the path of the suprascapular nerve. (**c**) Rotating the fixed-angle baseplate to achieve appropriate superior screw positioning causes the inferior screw to miss the scapular pillar completely (*black asterisk*) (Reprinted from Humphrey et al. [48] with permission from Elsevier)

Parsons et al. studied the effect of the rotation of the glenoid baseplate used in reverse total shoulder arthroplasty on screw fixation [79]. They implanted the baseplate into 12 cadaver scapulae in neutral rotation where the superior and inferior screw lined up with the 12 o'clock and 6 o'clock

positions. Then they rotated the baseplate 20° toward the base of the coracoid and 20° the opposite direction toward the spine of the scapula. The baseplates rotated toward the spine of the scapula had the shortest screws, and the baseplates rotated toward the base of the coracoid and neutral rotation resulted in the longest screws. Interestingly, the angle of the screw also affected the length of the screw. Perpendicular placement for the inferior screw yielded better results than an inferior angle. Perpendicular placement also allowed for similar lengths in screws for the superior screw when the baseplate was rotated toward the coracoid or in neutral rotation.

Stephens et al. evaluated the 73 scapulae using three-dimensional CT scans to determine the best rotation of the glenoid baseplate used for a reverse total shoulder that would allow for variable screw fixation into the three pillars of bone in the scapula body [90]. The optimal rotation of the baseplate was 11° anterior, which corresponds to rotating the superior hole of the baseplate toward the base of the coracoid. The average length of the superior and inferior screws was 33 mm.

Scapular neck length is a relatively new anatomic description that is taken on more interest with the recognition of scapular notching seen after reverse total shoulder replacement [93]. Paisley et al. evaluated the scapular neck length in a series of patients who underwent reverse total shoulder arthroplasty, and they found a significantly higher rate of notching in patients who had a scapular neck length less than 9 mm [77] (Figs. 6.12 and 6.13).

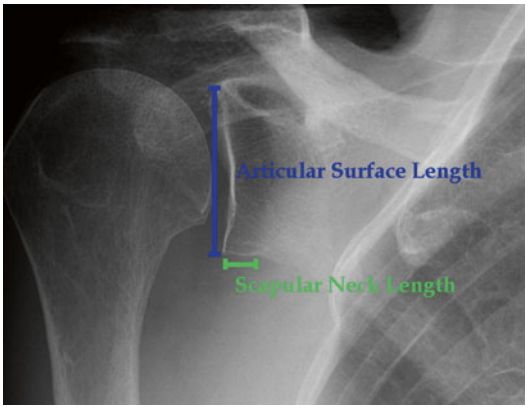

Fig. 6.12 Radiograph showing short scapular neck length (Reprinted from Paisley et al. [77] with permission from Elsevier)

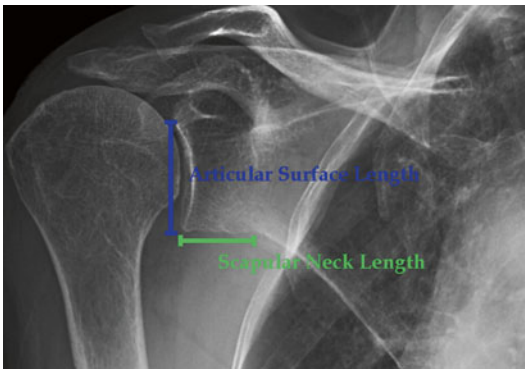

Fig. 6.13 Radiograph showing long scapular neck length (Reprinted from Paisley et al. [77] with permission from Elsevier)

Glenoid Pathology

Walsh et al. described one of the most commonly used glenoid classification systems to describe the different wear patterns seen in osteoarthritis of the shoulder [96]. Type A glenoids are characterized as having the humeral head in the center of the glenoid. Type A1 glenoids have minor central erosions, and type A2 glenoids have major central erosions. Type B glenoids are characterized by subluxation of the humeral head by more than 5 % of the diameter of the humeral head. Type B1 glenoids have subluxation of the humeral head with narrowing of the joint space with osteophytes and sclerosis. Type B2 glenoids have posterior erosions of the glenoid that result in a biconcave articular surface. Type C glenoids are characterized as having retroversion greater than 25°, regardless of the extent of the erosion (Fig. 6.14). This classification system has been studied and validated as a reliable classification system with the same interobserver reliability as other orthopedic classifications [70, 86].

Seebauer et al. described another classification system for the pathology of the glenoid that

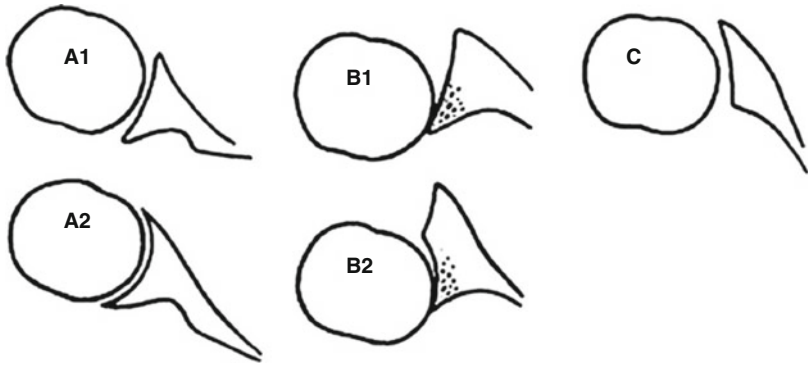

Fig. 6.14 Walch classification of glenoid erosion in primary glenohumeral arthritis (Reprinted from Walch et al. [96] with permission from Elsevier)

often occurs with rotator cuff tear arthropathy [95]. Type 1A cuff tear arthropathy has minimal superior migration of the humeral head, so the glenoid has minimal pathologic changes. Type 1B cuff tear arthropathy is characterized by minimal superior migration of the humeral head with medial and centralized glenoid erosion. Type 2A cuff tear arthropathy is characterized by superior translation of the humeral head with superior erosion of the glenoid. Type 2B cuff tear arthropathy is characterized by superior escape of the humeral head through the CA arch restraints.

Glenoid dysplasia is another pathologic disease that causes significant deformity of the glenoid [89]. These glenoid deformities fall under the category of a Walsh type C glenoid. The glenoids have decreased bone inferior and posterior, and the coracoid is typically very prominent. The posterior labrum can be hypertrophic. The humeral head usually has some form of dysplasia as well, and it is often subluxated posteriorly. As the disease progresses, the joint becomes arthritic, and this can occur at an early age.

Antuna et al. described a classification system to describe the different types of glenoid bone loss that typically occur after the removal of a glenoid implant [4]. The first type of defect is centralized, and it can be further characterized into mild, moderate, and severe. The second type of defect is characterized by some defect in the periphery of the glenoid or a defect in the glenoid walls. This can also be further characterized as mild, moderate, or severe. The third type of defect is a combined central defect that extends out to the walls of the glenoid vault. This can also be characterized as mild, moderate, or severe (Fig. 6.15).

Glenoid Implant Options

The glenoid implant is difficult to design because of the relatively small amount of bone available for the implant. Glenoid implant loosening is the most common complication of a total shoulder arthroplasty, so the majority of the research done to improve total shoulder arthroplasty has focused on the biomechanics and design of the glenoid implant. Earlier designs of the glenoid implant were fixed to the bone with cement, and this method continues to be the gold standard for glenoid implant design. In an attempt to improve the fixation strength of the implant, metal backings were added to the implant to allow for screw fixation into the glenoid and scapula. Biomechanical studies on the initial fixation of these designs showed great promise, but due to the altered mechanics specific to metal-backed glenoid implants of the total shoulder, these early designs failed at a higher rate than the traditional cemented all-polyethylene designs. The next generation of glenoid design included methods to incorporate bone ingrowth into the implant in addition to cement in an effort to minimize the use of cement in the hopes that the long-term fixation could be improved. Several companies have a slightly different hybrid method for glenoid fixation. It is important to understand

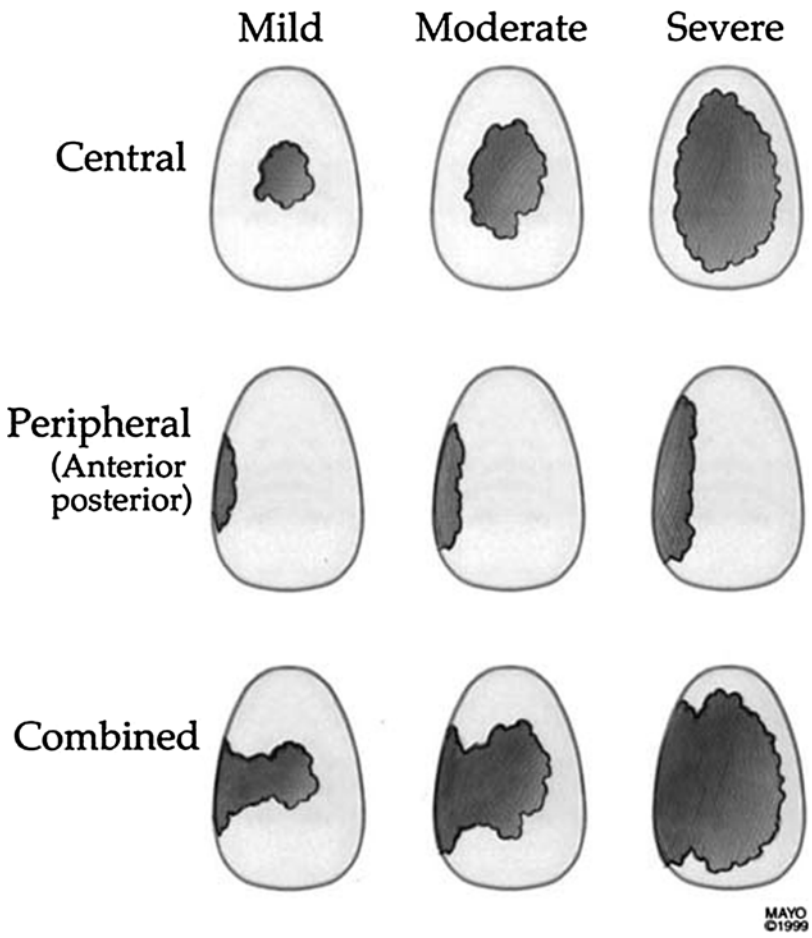

Fig. 6.15 Classification of bone deficiencies in the glenoid after glenoid component loosening and osteolysis. Most deficiencies are central or combined (Reprinted from Antuna et al. [4] with permission from Elsevier)

the differences in fixation among all the choices on the market and how the fixation is studied in the lab and in clinical studies.

Besides fixation design for glenoid implants, there are other considerations to take into account that may affect the long-term survival of the glenoid implant. The radius of curvature of the glenoid and its relationship to the humeral head radius of curvature, also described as the radial mismatch, can influence glenoid loosening during clinical follow-up. The alignment of the glenoid in terms of the version and inclination of the implant has an impact on the fixation of the implant and the forces that can potentially lead to early loosening of the implant. Bone quality is another factor that can affect the stability of the glenoid implant, and the difference in support that the subchondral bone can give compared to the softer cancellous bone found more medial in the glenoid vault may play a big role in the long-term stability of the glenoid implant. This can be a complicated decision-making process because the more a surgeon wants to correct the alignment of the pathologic glenoid to maximize the biomechanical stresses on the glenoid implant, the stronger the subchondral bone that must be removed to correct that alignment. The geometry of the backside of the glenoid implant can also influence the stability and long-term survival of the implant. Some implants have a flat back, and others have a curved backside of the implant. The radius of curvature of the backside of the implant can also play a role in both the stability of the implant to resist early loosening, and it can influence the amount of bone that is removed during the reaming process. The closer the geometry of the backside of the implant matches the geometry of the articular

surface of the glenoid, the less bone that will need to be removed during the surgery.

A final design consideration that can affect the long-term survivorship of the glenoid implant is the type of ultrahigh-molecular-weight polyethylene that is used for the material of the implant. The amount of cross-links in the polyethylene can change the biomechanical strength of the material to resist shear forces and friction forces [100].

Biomechanics of Glenoid Implants

Glenoid component loosening is the most common complication of total shoulder arthroplasty, so it is important to use laboratory testing of new designs before they are used in a clinical setting. Once a standard testing method is designed, then the different designs of implants can be compared and the effect of the individual factors can be determined. Anglin et al. described a method to test glenoid implants that is now the current standard adopted by ASTM International [2]. Their method was based on the clinical descriptions of glenoid implant failure by other investigators who thought the major contributing factor to glenoid loosening was off-center or eccentric loading of the implant. Off-center loading of the glenoid is caused by migration of the humeral head in one direction, often caused by a rotator cuff tear. Tears of the supraspinatus are the most common and can result in superior migration of the humeral head and eccentric loading of the superior glenoid. The same effect can occur when the subscapularis tendon is torn, which would result in migration of the humeral head anteriorly. Soft tissue imbalance can be another cause, which is often seen after instability surgery where the anterior soft tissue is less compliant compared to the posterior structures. Malposition of the glenoid component with excessive superior inclination can also contribute [54]. Bone deformity and subluxation of the humeral head can lead to an imbalance of the humeral head after a total shoulder if the surgeon cannot balance the humeral head with the appropriate releases and implant selection. This can then lead to eccentric loading of the posterior edge of the glenoid implant. The common term that is used to describe this eccentric loading is the "rocking horse" phenomenon, and it is the basis for testing standard that Anglin et al. described.

A biaxial apparatus was made that allowed constant compression of the humeral head into the glenoid implant (Fig. 6.16). Then the glenoid implant was moved until the center of the humeral head was over the edge of the glenoid rim. The direction of the glenoid movement was then changed until the humeral head moved to the other side of the glenoid rim. Multiple cycles were performed to simulate the 25 high-load activities a day such as lifting a briefcase or pushing on a chair to stand up over a 10-year period. The displacement of the glenoid rim during and after the cycles was measured to determine the stability of the construct. The investigators used this testing method to compare glenoid implants with the following variables: (1) flat backed, (2) curve backed, (3) keel, (4) two pegs, (5) four pegs, (6) smooth or rough backed, and (7) conformity between the humeral head and glenoid radius of curvature. The results showed less micromotion for the rough-backed glenoids compared to the smooth-backed glenoids due to less debonding of the cement from the backside of the implant. The curve-backed glenoids also had half the micromotion compared to the flat-backed glenoids. The less conforming radius of curvature had less micromotion compared to the implants with a more conforming radius of curvature.

Glenoid Cementing

Cement is currently the most common fixation method for a glenoid implant, and there have been several studies on cementing technique to improve the fixation and stability of the implant. Nyffeler et al. conducted a study to determine the best glenoid implant design of the implant pegs [72]. They used pullout tests rather than cyclical loading tests described by Anglin et al. They found that the threaded pegs had a higher pullout strength than the notched pegs and that the smooth pegs had the least resistance to pullout. The cement mantle thickness around the pegs was also studied, and

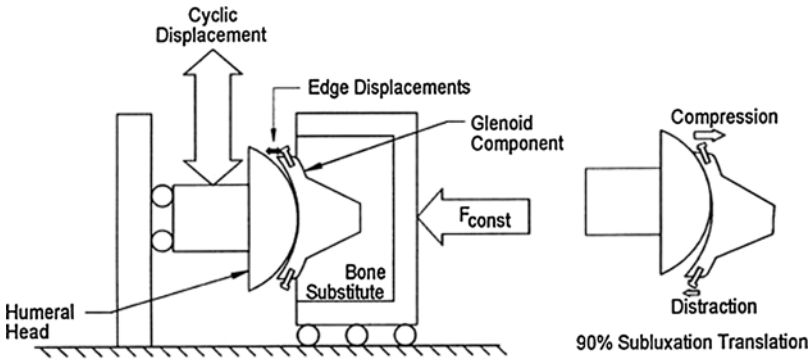

Fig. 6.16 Schematic of the biaxial testing apparatus. The humeral head was compressed into the glenoid with 750 N, then vertically translated inferiorly and superiorly to 90 % of the predetermined subluxation distance to mimic the rocking-horse phenomenon. The corresponding compression and distraction displacements of the glenoid were measured before and after 100,000 cycles (Reprinted from Anglin et al. [2] with permission from Elsevier)

they found that a mantle of 0.6 mm showed a significantly higher pullout strength than a cement mantle of 0.1 mm. Furthermore, a cement mantle of 0.1 mm usually resulted in a nonuniform thickness around each peg.

As mentioned above, Anglin et al. studied the effect of the backside geometry of the glenoid and found that a smooth-backed glenoid would quickly debond from the cement after only one cycle of loading. Nyffeler et al. studied the effect of cementing technique on the fixation of pegged glenoid implants [74]. One implant was fixed in cadavers using a syringe to inject cement into the peg holes, and cement was covered on the backside of the implant before it was implanted. Another set of cadavers was prepared by packing the cement with a finger into the peg holes. Cement was not placed on the backside of the implants. Micro-CT scans were taken to evaluate the cement mantle and the implant support by either bone or cement. The results showed a more uniform cement mantle around all the pegs when a syringe was used to fill the peg holes. The backsides of the implants were better supported with cement when the backside of the implant was covered with cement prior to implantation. More importantly, the glenoid implants were not uniformly supported by bone or cement, and some specimens had residual cartilage under the implant. This suggests that in vivo preparation of the glenoid, with the limits of surgical exposure, surgeon variability, and variability of the reamers used to prepare the glenoid, will result in an imperfect surface between the implant and the bone. Cement can fill those imperfections and support the glenoid, but there is a risk that the thin cement mantle could fragment.

In order to determine the quality of the cement technique used during surgery, and to determine whether the glenoid implant fixed with cement was loosening over time, a classification system was developed to evaluate the cement on postoperative x-rays [30]. Franklin et al. evaluated seven cases of total shoulder arthroplasty with irreparable rotator cuff tears and compared the x-rays to a control group of total shoulder replacements that did not have a rotator cuff tear. They described a tipping of the glenoid implant superiorly in the group of patients with a rotator cuff tear that was not seen in the control group. They described a radiographic grading system that was further modified by Lazarus et al. in a study that included 493 total shoulder replacements [63]. The grading system had two parts. The first part graded the radiolucency around the pegs of the glenoid implant, and the second part graded the completeness of glenoid component seating on the glenoid bone. They found radiolucencies about the glenoid component on initial radiographs in 308 of the 328 shoulders. They also found incomplete seating in a large number of shoulders, with incomplete posterior seating being the most common pattern (Tables 6.3 and 6.4). Other classification systems have been used as

Table 6.3 Lazarus grading scale for radiolucencies around a pegged glenoid implant

Grade	Description
0	No radiolucency
1	Incomplete radiolucency around one or two pegs
2	Complete radiolucency around one peg only, with or without incomplete radiolucency around one other peg
3	Complete radiolucency less than 2 mm wide around two or more pegs
4	Complete radiolucency more than 2 mm wide around two or more pegs
5	Gross loosening

Table 6.4 Grading scale for completeness of glenoid component seating

Grade	Description
A	Complete implant seating
B	<25 % incomplete contact, one x-ray
C	25–50 % incomplete contact, one x-ray
D	<50 % incomplete contact, two x-rays
E	>50 % incomplete contact, one x-ray

well [8, 15, 34, 102]. The clinical findings were further validated in a finite element analysis [46]. Malalignment of the glenoid component in the superior inferior plane provided the worst configuration for cement mantle stresses, and the quality of the supporting bone significantly affected the survivability of the cement mantle.

Klepps et al. studied the effect of using a syringe to deliver cement along with mechanical compression of the cement prior to seating of the implant, and they found similar improvements compared to manual finger packing of cement into the peg holes [56]. Barwood et al. studied the effect of cement pressurization and radiolucent lines on early postoperative radiographs [6]. The authors used a mechanical compression device to compress the cement into the peg holes, and this resulted in 90 % of the glenoid implants having zero radiolucencies around the pegs. Choi et al. compared the early postoperative radiographs of glenoid implants that were placed with two different cementing techniques [18]. The first series of implants were cemented with finger packing of the peg holes. The second series of glenoid implants were cemented using a syringe to fill the peg holes, followed by an impaction tool to compress the cement in the holes, followed by finger packing of doughy cement in the peg holes before the implant was put in place. No cement was placed on the backside of the implant. The radiolucent line score was greater than 1 in 45 % of the unpressurized group compared to 19 % in the pressurized group.

In an effort to improve the preparation of the glenoid peg holes for the glenoid implant, Edwards et al. evaluated three different drying techniques of the peg holes prior to insertion of the cement [27]. Twenty-one patients had the peg holes soaked in thrombin, 24 patients had the peg holes dried with compressed carbon dioxide, and 26 patients had the peg holes washed with saline and dried with sponges. The postoperative x-rays were compared among the three groups, and there was no statistical difference found. Forty-one percent of all the glenoids had radiolucency in at least one zone.

Another technique that has been described to improve the cementing technique for the glenoid was originally described for the implantation of stemmed components into the femur. Gross et al. studied the effect of creating a weep hole in the glenoid to allow excess air between the cement and the bone to escape and to allow application of suction to the glenoid vault to pull the cement into the vault [35]. The authors used postoperative x-rays to determine that the amount of cement around the pegs and the keel inside the vault was significantly larger than the glenoid implanted without the weep hole.

Peg vs. Keel

Biomechanical studies have been done in the lab to determine whether pegged or keeled glenoid implants conferred better stability to the implant. Wirth et al. implanted keeled and pegged glenoid implants into dogs and then tested the resistance to axial pullout of the implants after 0, 3, and 6 months [101]. The keeled implant had less resistance to pullout stress than the pegged implants. The radiographic and histologic examination showed partial or complete radiolucent

lines around the keel in each dog, which correlated with the mechanical testing results.

Lacroix et al. studied the failure of fixation of keeled and pegged glenoid components using finite element analysis [61]. They implanted a keeled component and a pegged component into cadaver bone using cement. The stresses around the cement were calculated, and they found that pegged implants had less failure when normal bone was used. When the bone was modified to mimic the structure of a patient with rheumatoid arthritis, the keeled implant had less failure of the cement mantle.

Multiple clinical studies have been done to determine the effect of the keel and peg design of the glenoid component. Gartsman et al. randomized 23 patients to receive a keeled glenoid component and 20 patients to receive a pegged glenoid component [34]. Postoperative radiographs were obtained at 6 weeks from the surgery, and radiographic lucency around the implant was measured. The pegged implants had a mean radiolucency score of 0.5, and the keeled implants had a mean radiolucency score of 1.4. Thirty-nine percent of the keeled components had a radiolucency score greater than 2, while only 5 % of the pegged components had a radiolucency score above 2.

Edwards et al. compared the results of pegged and keeled implants in a randomized study [26]. Fifty-three patients were randomized to each group, and the radiographs during the immediate postoperative period and at an average of 26 months after surgery were compared. The radiolucencies during the immediate postoperative period were 15 % in the keeled group compared to 0 % in the pegged group. After an average of 26 months, 46 % of the keeled implants had radiolucencies compared to 15 % in the pegged implant group. The strengths of this study included the fact that it was randomized so the selection bias, often attributed to the use of keel implants for the most challenging cases, was controlled. The same modern cementing techniques were used in both groups.

Lazarus et al. reviewed 328 postoperative shoulder radiographs and found a statistical trend toward a better result for pegged glenoid implants [63]. When the 0–5 scale was used, the keeled components were more likely to have a grade of 2 or greater when compared to the pegged implants.

Nuttall et al. used a different approach to measuring loosening of the glenoid component [71]. Rather than using radiolucency scores like other studies in the past, the group measured the micromotion of the implants over time using radiostereometric analysis. Beads were placed in five different locations around the scapula during surgery, and four beads were embedded into the keeled and pegged glenoid components. Stereoradiographs were obtained at multiple time points for the first 2 years after surgery. The highest maximum total point movement was 2.57 mm for the keeled components and 1.64 mm for the pegged components. All the components rotated into anteversion, 4.5° for the keeled components and 2.3° for the pegged components.

In contrast, Rahme et al. studied the stability of pegged and keeled glenoid components using radiostereometric analysis in 28 patients [81]. After 2-year follow-up, the authors did not find a difference in motion between the pegged and keeled glenoid components.

A more recent meta-analysis by Vavken et al. reviewed eight studies with a total of 1,460 patients that underwent total shoulder replacement with pegged and keeled components [94]. They found no significant difference in the risk of any radiolucency (risk ratio, 0.42; 95 % CI, 0.12–1.42) or in the risk of severe radiolucency (risk ratio, 0.65; 95 % CI, 0.23–1.82). The risk of revision was 0.27 (95 % CI, 0.08–0.88) in favor of pegged components ($p = 0.028$).

Radial Mismatch

The radii of the humeral head and the glenoid are not the same in the normal shoulder, and this radial mismatch has important effects on the biomechanics of the glenoid component in total shoulder arthroplasty. There is more conformity in the superior-inferior direction compared to the anterior-posterior direction in the normal shoulder [67]. When the mismatch between the humeral head and the glenoid component is low, there is

more conformity of the articular surface. This conformity makes the joint more stable, but it also increases the stress applied to the glenoid component during normal shoulder joint motion. Anglin et al. compared the displacement of a glenoid with radial mismatch of 1.77 mm to a glenoid with a mismatch of 5 mm and found that the displacement was half as much in the 5 mm mismatch group [3]. When the mismatch is higher, the stress over the entire glenoid is less during shoulder motion, but the point contact stress is higher. This point contact stress can impact the structure of the glenoid component and leads to earlier mechanical wear of the polyurethane. When the mismatch becomes too high, the humeral head can translate to the edge of the glenoid component and increase the risk of eccentric loading of the implant, a phenomenon described as the rocking horse effect by Franklin et al. [30].

Many implant designs incorporate a radial mismatch into the system in order to mimic the normal glenohumeral joint mechanics, and the amount of mismatch has been studied in both clinical and biomechanical studies. One of the most important studies that has been published on this topic was done by Walch et al. who evaluated the results of 319 total shoulder arthroplasties [97]. They divided the patients into four groups based on the amount of radial mismatch: (1) <4 mm, (2) 4.5–5.5 mm, (3) 6–7 mm, and (4) >7 mm. They evaluated the radiographs of these patients postoperatively at a mean follow-up of 54 months, and they found a linear relationship between the amount of radiolucencies around the implants and the amount of radial mismatch. The authors recommended that the amount of radial mismatch should be between 6 and 7 mm to obtain optimal results.

Radial mismatch is also another way to describe joint congruity. The more mismatch between the humeral and glenoid radius of curvature, the less congruity of the system. This is different than joint constraint, which is determined by the wall height of the glenoid component. One negative effect of increasing the radial mismatch is the potential for joint instability. Karduna et al. evaluated the effect of articular surface conformity on glenohumeral joint stability [53]. They controlled the effect of constraint by using the same glenoid component for each experiment, and they used different humeral head sizes to test the effect of varying conformity or radial mismatch of the system. The authors found that variations in joint conformity only accounted for 3 % of the force needed to dislocate the joint. In other words, increasing radial mismatch did not lead to increased risk of dislocation as long as the constraint or wall height of the glenoid implant is unchanged.

In order to better define the amount of radial mismatch that will minimize micromotion of the glenoid component, Sabesan et al. tested multiple size configurations of a cemented pegged all-polyethylene glenoid component [85]. The glenoids were loaded cyclically using the ASTM standard testing configuration described earlier, and the micromotion of the glenoids was measured. The micromotions of the implants with a radial mismatch of +2, +6, and +10 were not statistically different. The implants with a +14 and +18 mm mismatch could not complete the 50,000 cycles because of catastrophic failure. These results suggest that radial mismatch should be 10 mm or less.

Metal-Backed Glenoids

In an effort to improve the fixation of the all-polyethylene glenoid component, engineers developed polyethylene components that were fixed to the glenoid with some form of metal backing [80]. Earlier designs incorporated a metal platform that was secured to the glenoid with screws. This often resulted in an implant that was thicker than the all-polyethylene components, which had the potential to lateralize the joint line. Lateralization of the joint line can result in overstuffing of the joint, which in turn will alter the mechanics of the rotator cuff and lead to weakness or loss of shoulder motion. The lateralization can also increase the joint reactive forces that contribute to edge loading of the glenoid component, leading to wear of the polyethylene or premature loosening [78].

The material properties of the titanium metal, which is often used, have a different stiffness

than the bone or the polyethylene. The Young's modulus of titanium is >100 GPa, while the Young's modulus of bone is <10 GPa, and even lower is the Young's modulus of polyethylene <1 GPa. The differences in stiffness at the interfaces among the materials can lead to increased motion and wear of the softer polyethylene. The higher stiffness of the metal can also lead to stress shielding of portions of the glenoid bone, which risks loss of critical bone support that can already be small.

One of the first biomechanical studies that evaluated the stresses around a glenoid implant was done by Orr et al. [76]. The authors performed a two-dimensional finite element analysis to determine how a metal-backed glenoid component would change the stresses on the native glenoid compared to its normal state. The authors found that a metal implant similar to the Neer II system decreased the subchondral stresses, which explain why a metal-backed glenoid implant could cause osteolysis behind the implant. Another finite element analysis by Friedman et al. showed that an all-polyethylene component provides more physiologic stress distributions under nonaxial loading compared to metal-backed implants [32]. Stone et al. used the above data and performed an analysis using an all-polyethylene component and metal-backed component from the Cofield Total Shoulder System (Smith Nephew Richards, Inc, Memphis, Tenn). Using a two-dimensional finite element analysis, the authors found that the metal-backed implants reduced the subchondral bone stress, and this was more pronounced during eccentric loading [92].

Further biomechanical studies have shown that metal-backed glenoid implants have more stress concentration between the transition zone of the polyethylene and the metal [36]. They also show less stress at the metal-bone interface, which can explain the stress shielding and early failures seen in clinical follow-up studies [62].

Porous tantalum backing of the glenoid component was investigated by Andreykiv et al. [1]. Finite element models were used to determine the effect of porous tantalum on initial fixation, elastic properties of the implant, and friction at the bone-implant interface. The authors found that the major role of the tantalum backing was not to firmly fix the prosthesis but, instead, to distribute the load across the entire area of the bone-implant interface, which will limit the micromotion and allow for optimal bone ingrowth.

Zimmer, Inc. introduced a porous tantalum-backed glenoid component, and the initial fixation of the implant was compared to an all-polyethylene glenoid component by Budge et al. [12]. The tantalum implant was fixed to polyurethane bone substitute with a press-fit technique, PMMA cement, or calcium phosphate cement. The implants were loaded with the ASTM testing protocol, and glenoid distraction, compression, and translation were measured. The all-polyethylene implant fixed with cement demonstrated the least amount of micromotion, followed by the tantalum implant fixed with polymethyl methacrylate cement. A 2-year clinical follow-up study of tantalum-backed glenoid components was presented by the same research group, and they found a surprising number of early failures due to catastrophic dissociation between the polyethylene and tantalum keel [14].

Posterior Glenoid Bone Loss

One of the most challenging glenoid deformities to treat during total shoulder replacement is posterior glenoid bone loss that is often seen with Walch type B2 or C glenoids. Clinical studies have shown worse results for total shoulder arthroplasty in patients with posterior glenoid bone loss [51, 64]. The options to treat these types of glenoids include correction of retroversion of the glenoid by reaming the "high side" of the anterior glenoid bone, implantation of the glenoid component in retroversion, implantation of an augmented glenoid component, correction of the posterior bone loss with bone graft, hemiarthroplasty, or reverse total shoulder arthroplasty [47, 91]. Reaming the high side of the glenoid to correct the retroversion of the glenoid is the most commonly used technique to correct glenoid version, but it can lead to medialization of the joint line and perforation of the implant pegs [20, 69, 84]. This technique can also take

away the strong subchondral bone anteriorly, which may compromise the long-term fixation of the glenoid component. Medialization of the joint line or incomplete correction of the retroversion can also lead to posterior instability of the humeral head or early loosening of the glenoid component [42, 44]. When the posterior bone loss is severe, reaming of the glenoid with any technique may still leave a significant portion of the glenoid unsupported by bone. Reports of bone grafting the posterior glenoid showed some promise, but there are complications associated with the technique including early loosening of the glenoid implant and broken hardware [57, 83].

Augmentation of the posterior glenoid implant is another method used to treat glenoids with posterior bone loss. The glenoid component can be augmented with different types of geometry on the backside of the implant. The Depuy Step Tech implant uses a dual curved back design where the posterior and anterior portions of the implant have the same curved geometry at two different heights with a step in the middle. This requires removal of bone from the posterior and central portions of the glenoid, but this allows for better biomechanical resistance to micromotion compared to other backside geometries [50]. The Exactech posterior glenoid augment design has a curved backside with one curve designed to match the retroversion of the glenoid. The pegs are perpendicular to the articular surface, which is angled in relation to the backside of the glenoid so that the articular surface is aligned with the neutral version of the scapula. The benefit of this design is that it requires less bone removal, so it preserves the strong subchondral bone layer that may play an important role in the long-term survival of the implant [58]. The geometry of the backside of the implant may, however, lead to early loosening because it does not resist micromotion as well as other designs. Future designs will likely have even more variation in the design and geometry that impacts fixation and long-term survivorship. Hopefully, the results of biomechanical studies and clinical outcome studies can help surgeons make the best choice for each individual patient.

Bryce et al. studied the effect of posterior glenoid bone loss on humeral head translation [11]. They used eight cadaver scapulae and removed the posterior glenoid bone in 5° increments. The humeral head was loaded onto the glenoid in various positions, and the amount of humeral head translation was measured. They found that the humeral head translated posteriorly to a significant degree after 20° of posterior bone was removed when the humeral head was in neutral rotation. They also found that as little as 5° of posterior bone loss resulted in significant posterior humeral head translation when the humerus was in forward flexion. Five degrees of posterior bone loss equated to 2.5° of retroversion in this study.

Nyffeler et al. used a cadaver model to determine the effects of glenoid version on humeral head instability and glenoid component loosening [75]. They implanted a total shoulder into cadaver specimens and altered the glenoid component version in steps of 4°. The shoulders were loaded with physiologic loads, and the translation of the humeral head and the loads across the glenoid component were measured. They found that any retroversion of the glenoid component led to posterior translation of the humeral head and that small degrees of retroversion resulted in eccentric loading of the glenoid component that could result in early loosening. Furthermore, anteversion of the humeral head did not compensate for retroversion of the glenoid component.

To determine the risks of loosening of the glenoid component when it is implanted in retroversion, Farron et al. used a finite element model [28]. A keeled glenoid component was implanted into a normal glenoid in neutral version and 4 other positions of retroversion, 5°, 10°, 15°, and 20°. The model used a 1 mm layer of cement around the implant. Glenoid retroversion of 20° increased the peak cement stress by 326 % at the posterior part of the cement mantle. In the neutral position, the cement loads were evenly distributed around the keel and glenoid back. Micromotion increased with retroversion above 5°, and the maximal micromotion was +706 %. The stress of the glenoid bone was also increased +162 % when the implant was retroverted to 20°,

and this stress was localized at the posterior aspect of the glenoid.

Youngpravat et al. performed an elegant study that takes into account both the subchondral bone density and the orientation of the glenoid component in the case of posterior glenoid bone loss. The investigators used a homogenous bone model as well as a model with cortical and cancellous bone. The glenoid component was implanted with complete correction, partial correction, and partial component backside bone support. In the homogeneous bone model, complete correction with reaming of the high side bone resulted in the strongest configuration. Implantation of the glenoid component in retroversion without correction had the highest risk of failure. In the heterogeneous bone model, complete correction of the retroversion by reaming the high side of the anterior glenoid had the highest risk of failure [103] (Fig. 6.17).

Kirane et al. evaluated the biomechanical characteristics of an all-polyethylene and titanium step used to augment a polyethylene glenoid component in cadaver specimens [55]. The investigators created a posterior defect in the glenoid and implanted a pegged all-polyethylene implant augmented with either a polyethylene augment or a titanium augment. The control group for the experiment was a normal glenoid implant used in a normal glenoid without a posterior defect. Loads were applied through the

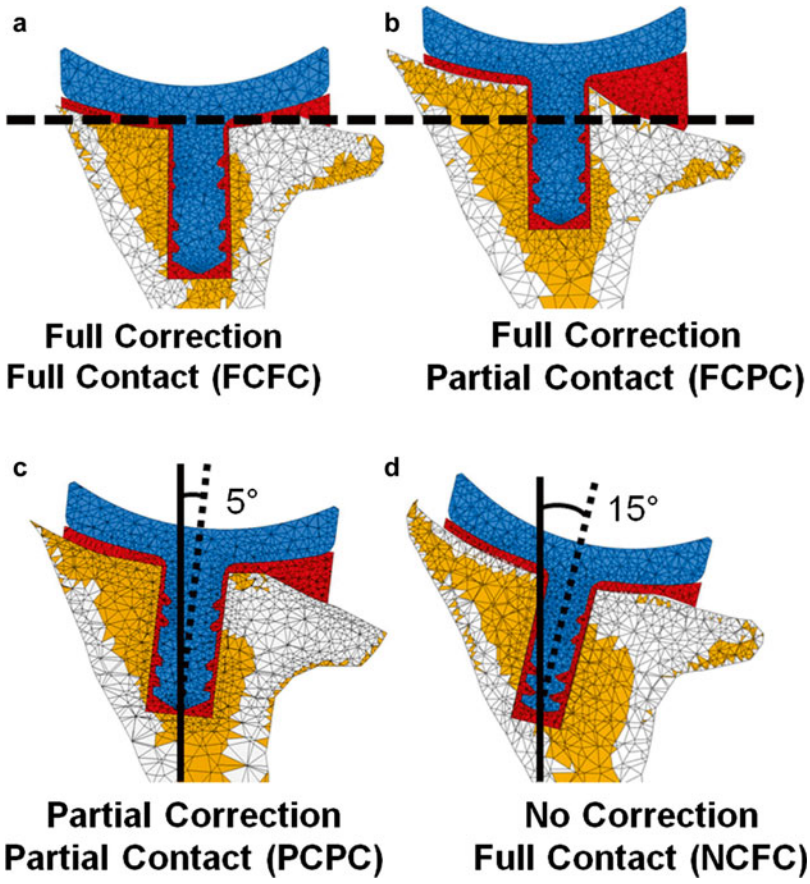

Fig. 6.17 Total shoulder arthroplasty scenarios are shown for study group 2 (heterogeneous scapula): (**a**) full correction, full contact (FCFC); (**b**) full correction, partial contact (FCPC); (**c**) partial correction, partial contact (PCPC); (**d**) no correction, full contact (NCFC). The *blue, red, white,* and *orange* indicate, respectively, implant, cement, cortical bone, and trabecular bone. Note the occurrence of glenoid decortication, particularly in the FCFC scenario, when correcting significant bony pathology (Reprinted from Yongpravat et al. [103] with permission from Elsevier)

rotator cuff muscles to simulate the force generated when a patient pushes his/her body weight away from a wall. The peri-glenoid strains recorded during the experiments were similar for the controls and the polyethylene augmented glenoid. The peri-glenoid strains were higher in the group augmented by the titanium augment.

Wang et al. compared the initial stability of standard all-polyethylene component that was prepared with eccentric reaming to correct retroversion to neutral with the initial stability of a posterior augmented all-polyethylene component with an 8° angle-backed posterior augment [99]. Cyclic loading was applied to all specimens according to the ASTM standard F2028-08 with 100,000 cycles. Superior and edge displacements were recorded during the loading protocol. Three of the six specimens in the posterior augmented group did not survive the loading protocol of the experiment, while five of the six implants in the eccentric anterior reaming group did survive the loading protocol. These data suggest that an angled-back geometry may not resist shear stress as well as the standard glenoid implant.

Iannotti et al. tested the biomechanical characteristics of four different glenoid designs with posterior augmentation with one non-augmented glenoid design [50]. The glenoids studied included the following types: (1) spherical asymmetric glenoid, (2) spherical symmetric glenoid, (3) flat angled glenoid, (4) stepped glenoid, and (5) standard symmetrical curved back glenoid. These glenoids all had the same central peg design (Fig. 6.18). The glenoid components were implanted into foam bone and cyclically loaded according to the ASTM standard protocol, and the micromotion of the anterior edge of the implant was measured. In the group that used cement for the peripheral pegs, after 100,000 cycles, the standard glenoid lift off was 34 ± 0 μ, the step tech was 87 ± 66 μ, the flat angled was 334 ± 179 μ, the spherical symmetric was 294 ± 174 μ, and the spherical asymmetric implant was 310 ± 23 μ. When the spherical symmetric design was compared to the step tech, there was a statistical difference at the initial loading of the implant, but there was not a statistically significant difference after 100,000 cycles.

Reverse Baseplate Fixation

Since the initial use of the reverse total shoulder, the glenoid component fixation has been a common reason for early implant failure. The first generation of reverse total shoulder designs used a lateralized center of rotation for the glenoid side of the implant. Modifications of the design

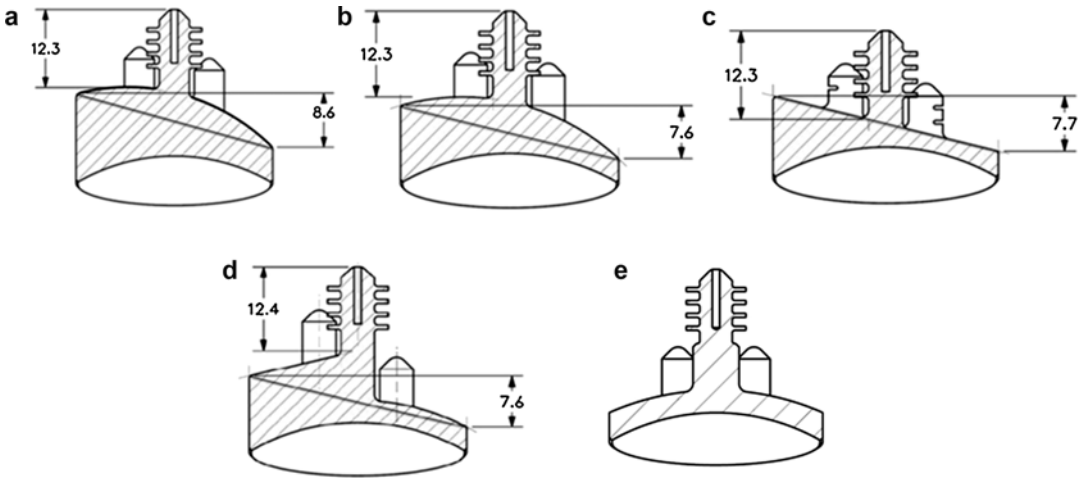

Fig. 6.18 Cross sections of five glenoid designs: (**a**) spherical asymmetric glenoid, (**b**) spherical symmetric glenoid, (**c**) flat angled glenoid, (**d**) stepped glenoid, and (**e**) Anchor Peg Glenoid (Reprinted from Iannotti et al. [50] with permission from Elsevier)

that medialized the center of rotation of the implant decreased the stresses of the glenoid baseplate and resulted in less loosening and less early failure [9]. New designs that allow for larger screws, locking screws, and variable screw angle insertion have improved the initial fixation of the glenoid baseplate as well. As the implant fixation methods have improved, implant designers have changed the center of rotation of the reverse constructs to more lateralized designs to help minimize the complications that occur with medialization. Some authors have described less scapular notching when the center of rotation is lateralized because the medial calcar of the humeral implant is less likely to impinge on the scapula [5, 59, 82, 88]. Other biomechanical considerations have improved the surgical technique used to insert the baseplate, and these have been tested in biomechanical studies. Some modifications that are more difficult to test in the lab include bone ingrowth technology. These biologic solutions cannot be simulated with our current biomechanical experiments, so we must rely on long-term clinical follow-up before knowing how well these factors affect the stability of the glenoid baseplates.

Some of the earlier biomechanical studies focused on the effect of the screws used to fix the glenoid baseplate. Chebli et al. used a sawbone model to fix a glenoid baseplate with multiple variations in screw configurations [16]. The authors found that the inferior screw was the most important because fixation strength was 35 % weaker when that screw was omitted. The strength of the fixation was 16 % weaker if the superior screw was omitted. Harmen et al. compared the fixation of the Encore reverse baseplate fixation, which uses 4 locking screws and a central non-locking screw with a flat baseplate to the Depuy Delta III baseplate fixation, which uses two locking screws and two non-locking screws to fix a flat baseplate with a central peg [39]. The Encore design used a lateralized center of rotation which exerts a 69 % higher load onto the baseplate compared to the Delta III design that has a more medialized center of rotation. The micromotion of both designs was below the threshold of 150 μ that is required to obtain bone ingrowth into the implants. If the Encore baseplate was fixed with non-locking screws, the micromotion was above the 150 μ threshold.

The number of screws used to fix the glenoid has also become a question for debate as different designs use multiple screw configurations. All designs incorporate at a minimum a superior and inferior screw, which are commonly locked to the plate. Many designs also include a screw that can be fixed in the center of the glenoid baseplate that engages the cortical bone in the middle column of the scapula. Other designs allow for an anterior and posterior screw to be placed, but the bone can be thin and soft in these positions after the glenoid has been reamed, especially in smaller women. When the posterior screw engages both the glenoid cortex and the cortex of the scapular spine, the stability of the glenoid implant has been shown to improve significantly by two separate studies [23, 45]. The problem with using this type of configuration is that the screw can potentially injure the suprascapular nerve as it courses around the base of the scapular spine [40, 68, 98]. James et al. studied the effect of using two locking screws alone compared to two locking screws in addition to two non-locking screws in the anterior and posterior positions. They did not find any difference between the micromotion of the glenoid baseplate in their cadaver model [52].

It is often difficult to apply the results of one biomechanical study that uses a specific implant to another implant that may have other important design characteristics that influence initial fixation of the implant. These design differences include backside geometry such as flat-backed or curve-backed designs. Curved-backed designs have been showed to improve initial stability in biomechanical testing, but they have the disadvantage of removing more cortical bone on the inferior glenoid due to the more inferior positioning of the implant compared to an anatomic implant [52]. This inferior placement is done to avoid notching of the scapula by the medial calcar of the humeral implant. The inclination of the glenoid implant also plays a critical role in the initial fixation of the implant and the likelihood of causing of scapular notching. Some authors have shown that inferior tilt of the glenosphere improves the mechanics of the implant and decreases the micromotion in sawbone models

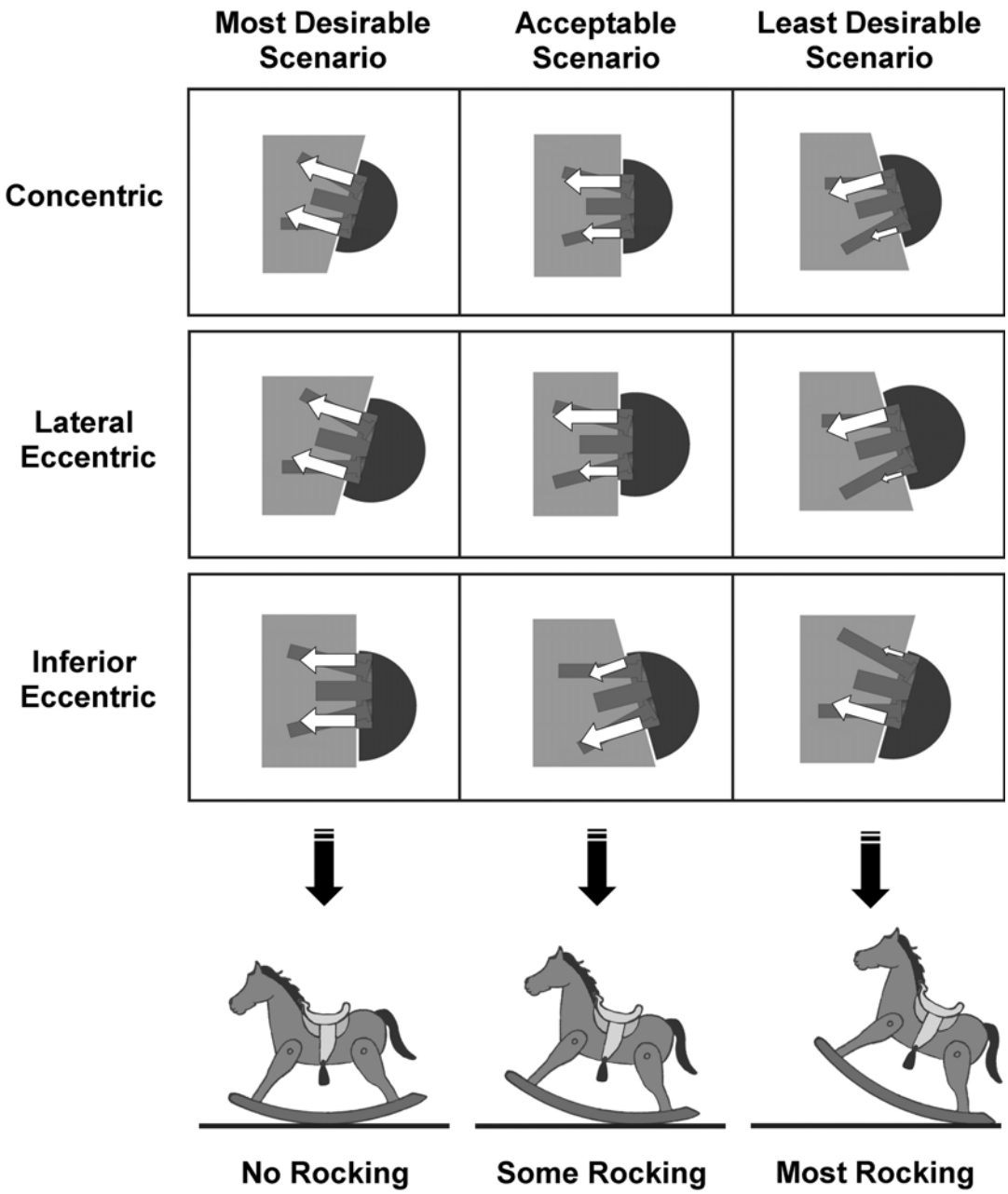

Fig. 6.19 This is an illustration of the effect of different forces at the baseplate-bone interface. Each glenosphere configuration (concentric, lateral eccentric, and inferior eccentric) can be placed in differing tilts to produce more even forces at the baseplate-bone interface. These forces are optimum for concentric and lateral eccentric glenospheres when placed in inferior tilt, while for inferior eccentric glenospheres, the optimal tilt is neutral; this placement will cause the least amount of rocking. The other tilts lead to more uneven forces at the baseplate-bone junction and hence, increased rocking (Reprinted from Gutierrez et al. [38] with permission from Elsevier)

[38]. In an effort to minimize notching that was often seen with medialized glenoid designs, the glenosphere was changed to allow for inferior eccentric placement of the glenosphere on the baseplate. This allows the humeral component to be pushed more inferior and allows for more clearance before the humerus could impinge on the scapula. The biomechanical effect of this

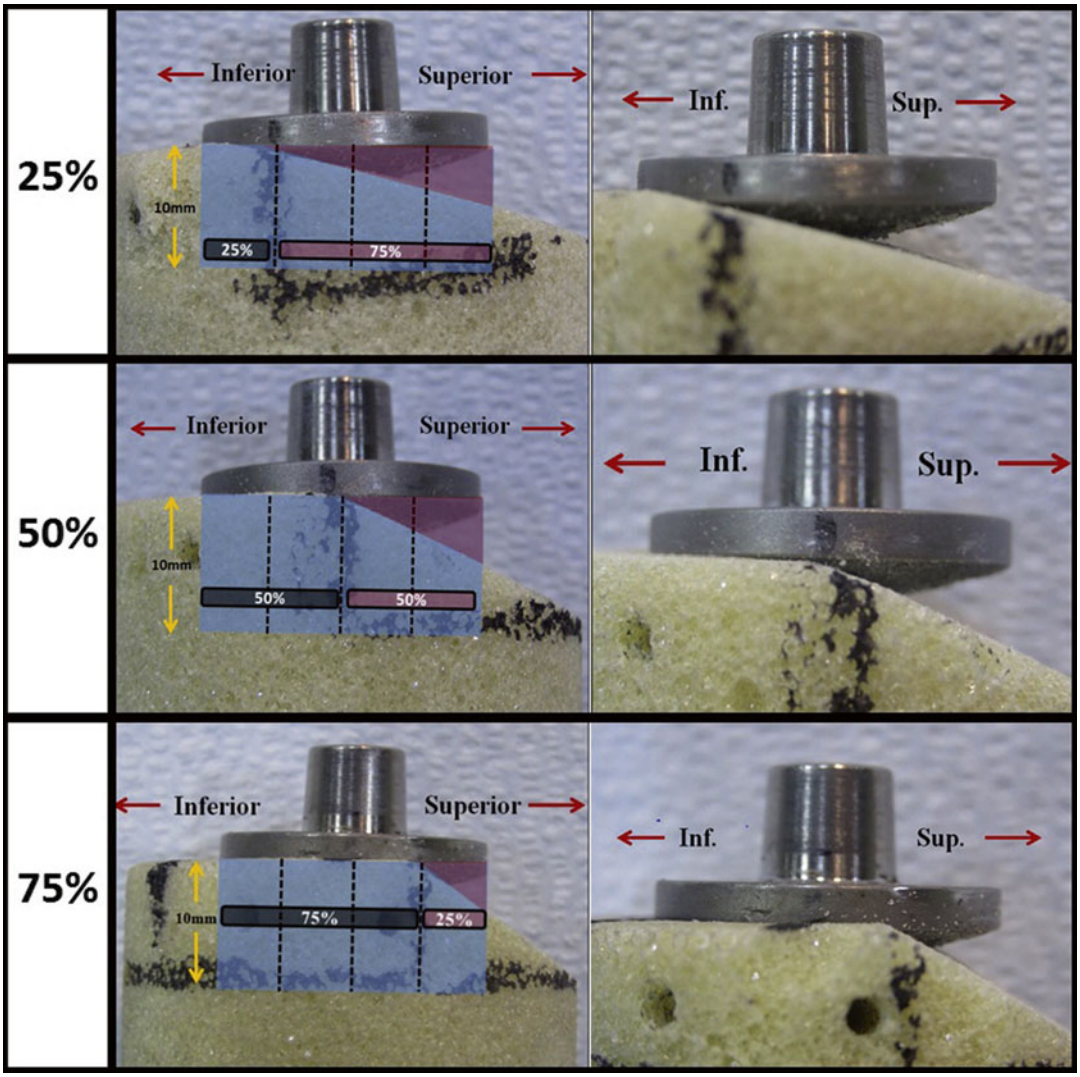

Fig. 6.20 Examples of the baseplate coverage experimental groups, demonstrating 25 % coverage, 50 % coverage, and 75 % coverage of the undersurface of the glenoid baseplate (100 % coverage not shown) (Reprinted from Formaini et al. [29] with permission from Elsevier)

design compared to the medialized concentric design and a lateralized design was studied by Gutierrez et al. They found better mechanics and less rocking horse potential when the concentric and lateralized design was placed with inferior tilt, but the eccentric design had the best biomechanical stability when it was placed without any tilt [37] (Fig. 6.19).

Bone loss can affect the stability of the reverse glenoid baseplate, and this is more commonly seen in difficult revision cases where the reverse total shoulder is used. Surgeons are also confronted with an intraoperative decision when reaming the glenoid with inferior tilt, a method shown to improve the stability of the implant. The surgeon often has to ream away good bone medially in order to achieve complete backside bone coverage of the baseplate. Should the surgeon stop reaming and implant the baseplate with 75 % or 50 % coverage, or continue to ream medially in order to obtain 100 % bone coverage of the baseplate? Formaini et al. tried to answer

this question, and they examined the effect of different levels of bone loss on the initial stability of the Encore reverse glenoid baseplate in a foam block model [29]. They found that the micromotion of the baseplate was above the 150 μ threshold needed for bone ingrowth, but that 50 %, 75 %, and normal glenoid bone conditions did not show any significant difference in micromotion (Fig. 6.20).

Summary

In summary, glenoid version can be accurately measured with axillary radiographs taken with good technique. CT scans can help get better version measurements in cases of glenoid deformity, and the method of image acquisition can affect the version measurements by 10° if not done properly. The shape of the glenoid vault can be used to predict the version of a glenoid before it was deformed with pathology. Glenoid retroversion is increased in patients with arthritis compared to patients without pathology of the glenohumeral joint. Stability of glenoid implants is improved when the implant is completely supported by subchondral bone, and the version of the implant is not retroverted. Glenoid cement should be applied with pressurization, and metal-backed glenoids used in anatomic total shoulders have shown a higher revision rate than polyethylene glenoids in multiple studies. Metal baseplates used in reverse total shoulders depend on a minimum of one screw in the inferior column, which provides the most resistance to micromotion, and one screw in the superior column of the scapula. The reverse total shoulder baseplate should not be implanted with any superior inclination, and at least 50 % of the backside of the implant should be supported by the bone.

References

1. Andreykiv A, Prendergast PJ, van Keulen F, Swieszkowski W, Rozing PM. Bone ingrowth simulation for a concept glenoid component design. J Biomech. 2005;38(5):1023–33.
2. Anglin C, Wyss UP, Pichora DR. Mechanical testing of shoulder prostheses and recommendations for glenoid design. J Shoulder Elbow Surg. 2000;9(4):323–31.
3. Anglin C, Wyss UP, Pichora DR. Shoulder prosthesis subluxation: theory and experiment. J Shoulder Elbow Surg. 2000;9(2):104–14.
4. Antuna SA, Sperling JW, Cofield RH, Rowland CM. Glenoid revision surgery after total shoulder arthroplasty. J Shoulder Elbow Surg. 2001;10(3):217–24.
5. Athwal GS, MacDermid JC, Reddy KM, Marsh JP, Faber KJ, Drosdowech D. Does bony increased-offset reverse shoulder arthroplasty decrease scapular notching? J Shoulder Elbow Surg. 2015;24(3):468–73.
6. Barwood S, Setter KJ, Blaine TA, Bigliani LU. The incidence of early radiolucencies about a pegged glenoid component using cement pressurization. J Shoulder Elbow Surg. 2008;17(5):703–8.
7. Bicknell RT, Patterson SD, King GJ, Chess DG, Johnson JA. Glenoid vault endosteal dimensions: an anthropometric study with special interest in implant design. J Shoulder Elbow Surg. 2007;16(3 Suppl):S96–101.
8. Boileau P, Avidor C, Krishnan SG, Walch G, Kempf JF, Mole D. Cemented polyethylene versus uncemented metal-backed glenoid components in total shoulder arthroplasty: a prospective, double-blind, randomized study. J Shoulder Elbow Surg. 2002;11(4):351–9.
9. Boileau P, Watkinson DJ, Hatzidakis AM, Balg F. Grammont reverse prosthesis: design, rationale, and biomechanics. J Shoulder Elbow Surg. 2005;14(1 Suppl S):147S–61.
10. Bryce CD, Davison AC, Lewis GS, Wang L, Flemming DJ, Armstrong AD. Two-dimensional glenoid version measurements vary with coronal and sagittal scapular rotation. J Bone Joint Surg Am. 2010;92(3):692–9.
11. Bryce CD, Davison AC, Okita N, Lewis GS, Sharkey NA, Armstrong AD. A biomechanical study of posterior glenoid bone loss and humeral head translation. J Shoulder Elbow Surg. 2010;19(7):994–1002.
12. Budge MD, Kurdziel MD, Baker KC, Wiater JM. A biomechanical analysis of initial fixation options for porous-tantalum-backed glenoid components. J Shoulder Elbow Surg. 2013;22(5):709–15.
13. Budge MD, Lewis GS, Schaefer E, Coquia S, Flemming DJ, Armstrong AD. Comparison of standard two-dimensional and three-dimensional corrected glenoid version measurements. J Shoulder Elbow Surg. 2011;20(4):577–83.
14. Budge MD, Nolan EM, Heisey MH, Baker K, Wiater JM. Results of total shoulder arthroplasty with a monoblock porous tantalum glenoid component: a prospective minimum 2-year follow-up study. J Shoulder Elbow Surg. 2013;22(4):535–41.
15. Carke IC, Sew Hoy AL, Gruen TA, Amstutz HC. Clinical and radiographic assessment of a non-constrained total shoulder. Int Orthop. 1981;5(1):1–8.

16. Chebli C, Huber P, Watling J, Bertelsen A, Bicknell RT, Matsen 3rd F. Factors affecting fixation of the glenoid component of a reverse total shoulder prosthesis. J Shoulder Elbow Surg. 2008;17(2):323–7.
17. Checroun AJ, Hawkins C, Kummer FJ, Zuckerman JD. Fit of current glenoid component designs: an anatomic cadaver study. J Shoulder Elbow Surg. 2002;11(6):614–7.
18. Choi T, Horodyski M, Struk AM, Sahajpal DT, Wright TW. Incidence of early radiolucent lines after glenoid component insertion for total shoulder arthroplasty: a radiographic study comparing pressurized and unpressurized cementing techniques. J Shoulder Elbow Surg. 2013;22(3):403–8.
19. Churchill RS, Brems JJ, Kotschi H. Glenoid size, inclination, and version: an anatomic study. J Shoulder Elbow Surg. 2001;10(4):327–32.
20. Clavert P, Millett PJ, Warner JJ. Glenoid resurfacing: what are the limits to asymmetric reaming for posterior erosion? J Shoulder Elbow Surg. 2007;16(6): 843–8.
21. Codsi MJ, Bennetts C, Gordiev K, Boeck DM, Kwon Y, Brems J, et al. Normal glenoid vault anatomy and validation of a novel glenoid implant shape. J Shoulder Elbow Surg. 2008;17(3):471–8.
22. Codsi MJ, Bennetts C, Powell K, Iannotti JP. Locations for screw fixation beyond the glenoid vault for fixation of glenoid implants into the scapula: an anatomic study. J Shoulder Elbow Surg. 2007;16(3 Suppl):S84–9.
23. Codsi MJ, Iannotti JP. The effect of screw position on the initial fixation of a reverse total shoulder prosthesis in a glenoid with a cavitary bone defect. J Shoulder Elbow Surg. 2008;17(3):479–86.
24. Couteau B, Mansat P, Mansat M, Darmana R, Egan J. In vivo characterization of glenoid with use of computed tomography. J Shoulder Elbow Surg. 2001;10(2):116–22.
25. Cyprien JM, Vasey HM, Burdet A, Bonvin JC, Kritsikis N, Vuagnat P. Humeral retrotorsion and glenohumeral relationship in the normal shoulder and in recurrent anterior dislocation (scapulometry). Clin Orthop Relat Res. 1983;175:8–17.
26. Edwards TB, Labriola JE, Stanley RJ, O'Connor DP, Elkousy HA, Gartsman GM. Radiographic comparison of pegged and keeled glenoid components using modern cementing techniques: a prospective randomized study. J Shoulder Elbow Surg. 2010; 19(2):251–7.
27. Edwards TB, Sabonghy EP, Elkousy H, Warnock KM, Hammerman SM, O'Connor DP, et al. Glenoid component insertion in total shoulder arthroplasty: comparison of three techniques for drying the glenoid before cementation. J Shoulder Elbow Surg. 2007;16(3 Suppl):S107–10.
28. Farron A, Terrier A, Buchler P. Risks of loosening of a prosthetic glenoid implanted in retroversion. J Shoulder Elbow Surg. 2006;15(4):521–6.
29. Formaini NT, Everding NG, Levy JC, Santoni BG, Nayak AN, Wilson C, et al. The effect of glenoid bone loss on reverse shoulder arthroplasty baseplate fixation. J Shoulder Elbow Surg. 2015;24:e312–9.
30. Franklin JL, Barrett WP, Jackins SE, Matsen 3rd FA. Glenoid loosening in total shoulder arthroplasty. Association with rotator cuff deficiency. J Arthroplast. 1988;3(1):39–46.
31. Friedman RJ, Hawthorne KB, Genez BM. The use of computerized tomography in the measurement of glenoid version. J Bone Joint Surg Am. 1992;74(7): 1032–7.
32. Friedman RJ, Laberge M, Dooley RL, O'Hara AL. Finite element modeling of the glenoid component: effect of design parameters on stress distribution. J Shoulder Elbow Surg. 1992;1(5):261–70.
33. Ganapathi A, McCarron JA, Chen X, Iannotti JP. Predicting normal glenoid version from the pathologic scapula: a comparison of 4 methods in 2- and 3-dimensional models. J Shoulder Elbow Surg. 2011;20(2):234–44.
34. Gartsman GM, Elkousy HA, Warnock KM, Edwards TB, O'Connor DP. Radiographic comparison of pegged and keeled glenoid components. J Shoulder Elbow Surg. 2005;14(3):252–7.
35. Gross RM, High R, Apker K, Haggstrom J, Fehringer JA, Stephan J. Vacuum assist glenoid fixation: does this technique lead to a more durable glenoid component? J Shoulder Elbow Surg. 2011;20(7):1050–60.
36. Gupta S, van der Helm FC, van Keulen F. Stress analysis of cemented glenoid prostheses in total shoulder arthroplasty. J Biomech. 2004;37(11):1777–86.
37. Gutierrez S, Greiwe RM, Frankle MA, Siegal S, Lee 3rd WE. Biomechanical comparison of component position and hardware failure in the reverse shoulder prosthesis. J Shoulder Elbow Surg. 2007;16(3 Suppl):S9–12.
38. Gutierrez S, Walker M, Willis M, Pupello DR, Frankle MA. Effects of tilt and glenosphere eccentricity on baseplate/bone interface forces in a computational model, validated by a mechanical model, of reverse shoulder arthroplasty. J Shoulder Elbow Surg. 2011;20(5):732–9.
39. Harman M, Frankle M, Vasey M, Banks S. Initial glenoid component fixation in "reverse" total shoulder arthroplasty: a biomechanical evaluation. J Shoulder Elbow Surg. 2005;14(1 Suppl S):162s–7.
40. Hart ND, Clark JC, Wade Krause FR, Kissenberth MJ, Bragg WE, Hawkins RJ. Glenoid screw position in the encore reverse shoulder prosthesis: an anatomic dissection study of screw relationship to surrounding structures. J Shoulder Elbow Surg. 2013;22(6):814–20.
41. Hendel MD, Bryan JA, Barsoum WK, Rodriguez EJ, Brems JJ, Evans PJ, et al. Comparison of patient-specific instruments with standard surgical instruments in determining glenoid component position: a randomized prospective clinical trial. J Bone Joint Surg Am. 2012;94(23):2167–75.
42. Ho JC, Sabesan VJ, Iannotti JP. Glenoid component retroversion is associated with osteolysis. J Bone Joint Surg Am. 2013;95(12), e82.

43. Ho JC, Youderian A, Davidson IU, Bryan J, Iannotti JP. Accuracy and reliability of postoperative radiographic measurements of glenoid anatomy and relationships in patients with total shoulder arthroplasty. J Shoulder Elbow Surg. 2013;22(8):1068–77.
44. Hoenecke Jr HR, Tibor LM, D'Lima DD. Glenoid morphology rather than version predicts humeral subluxation: a different perspective on the glenoid in total shoulder arthroplasty. J Shoulder Elbow Surg. 2012;21(9):1136–41.
45. Hoenig MP, Loeffler B, Brown S, Peindl R, Fleischli J, Connor P, et al. Reverse glenoid component fixation: is a posterior screw necessary? J Shoulder Elbow Surg. 2010;19(4):544–9.
46. Hopkins AR, Hansen UN, Amis AA, Emery R. The effects of glenoid component alignment variations on cement mantle stresses in total shoulder arthroplasty. J Shoulder Elb Surg. 2004;13(6):668–75.
47. Hsu JE, Ricchetti ET, Huffman GR, Iannotti JP, Glaser DL. Addressing glenoid bone deficiency and asymmetric posterior erosion in shoulder arthroplasty. J Shoulder Elbow Surg. 2013;22(9): 1298–308.
48. Humphrey CS, Kelly 2nd JD, Norris TR. Optimizing glenosphere position and fixation in reverse shoulder arthroplasty, Part two: the three-column concept. J Shoulder Elbow Surg. 2008;17(4):595–601.
49. Iannotti JP, Gabriel JP, Schneck SL, Evans BG, Misra S. The normal glenohumeral relationships. An anatomical study of one hundred and forty shoulders. J Bone Joint Surg Am. 1992;74(4):491–500.
50. Iannotti JP, Lappin KE, Klotz CL, Reber EW, Swope SW. Liftoff resistance of augmented glenoid components during cyclic fatigue loading in the posterior-superior direction. J Shoulder Elbow Surg. 2013; 22(11):1530–6.
51. Iannotti JP, Norris TR. Influence of preoperative factors on outcome of shoulder arthroplasty for glenohumeral osteoarthritis. J Bone Joint Surg Am. 2003; 85-A(2):251–8.
52. James J, Huffman KR, Werner FW, Sutton LG, Nanavati VN. Does glenoid baseplate geometry affect its fixation in reverse shoulder arthroplasty? J Shoulder Elbow Surg. 2012;21(7):917–24.
53. Karduna AR, Williams GR, Williams JL, Iannotti JP. Joint stability after total shoulder arthroplasty in a cadaver model. J Shoulder Elbow Surg. 1997;6(6): 506–11.
54. Karelse A, Van Tongel A, Verstraeten T, Poncet D, De Wilde LF. Rocking-horse phenomenon of the glenoid component: the importance of inclination. J Shoulder Elbow Surg. 2015;24(7):1142–8.
55. Kirane YM, Lewis GS, Sharkey NA, Armstrong AD. Mechanical characteristics of a novel posterior-step prosthesis for biconcave glenoid defects. J Shoulder Elbow Surg. 2012;21(1):105–15.
56. Klepps S, Chiang AS, Miller S, Jiang CY, Hazrati Y, Flatow EL. Incidence of early radiolucent glenoid lines in patients having total shoulder replacements. Clin Orthop Relat Res. 2005;435:118–25.
57. Klika BJ, Wooten CW, Sperling JW, Steinmann SP, Schleck CD, Harmsen WS, et al. Structural bone grafting for glenoid deficiency in primary total shoulder arthroplasty. J Shoulder Elbow Surg. 2014; 23(7):1066–72.
58. Knowles NK, Ferreira LM, Athwal GS. Augmented glenoid component designs for type B2 erosions: a computational comparison by volume of bone removal and quality of remaining bone. J Shoulder Elbow Surg. 2015;24(8):1218–26.
59. Kowalsky MS, Galatz LM, Shia DS, Steger-May K, Keener JD. The relationship between scapular notching and reverse shoulder arthroplasty prosthesis design. J Shoulder Elbow Surg. 2012;21(10): 1430–41.
60. Kwon YW, Powell KA, Yum JK, Brems JJ, Iannotti JP. Use of three-dimensional computed tomography for the analysis of the glenoid anatomy. J Shoulder Elbow Surg. 2005;14(1):85–90.
61. Lacroix D, Murphy LA, Prendergast PJ. Three-dimensional finite element analysis of glenoid replacement prostheses: a comparison of keeled and pegged anchorage systems. J Biomech Eng. 2000; 122(4):430–6.
62. Lawrence TM, Ahmadi S, Sperling JW, Cofield RH. Fixation and durability of a bone-ingrowth component for glenoid bone loss. J Shoulder Elbow Surg. 2012;21(12):1764–9.
63. Lazarus MD, Jensen KL, Southworth C, Matsen FA. The radiographic evaluation of keeled and pegged glenoid component insertion. J Bone Joint Surg Am. 2002;84-a(7):1174–82.
64. Levine WN, Djurasovic M, Glasson JM, Pollock RG, Flatow EL, Bigliani LU. Hemiarthroplasty for glenohumeral osteoarthritis: results correlated to degree of glenoid wear. J Shoulder Elbow Surg. 1997;6(5):449–54.
65. Mallon WJ, Brown HR, Vogler JB, 3rd, Martinez S. Radiographic and geometric anatomy of the scapula. Clin Orthop Relat Res. 1992;277:142–54.
66. Matsumura N, Ogawa K, Kobayashi S, Oki S, Watanabe A, Ikegami H, et al. Morphologic features of humeral head and glenoid version in the normal glenohumeral joint. J Shoulder Elbow Surg. 2014; 23(11):1724–30.
67. McPherson EJ, Friedman RJ, An YH, Chokesi R, Dooley RL. Anthropometric study of normal glenohumeral relationships. J Shoulder Elbow Surg. 1997; 6(2):105–12.
68. Molony DC, Cassar Gheiti AJ, Kennedy J, Green C, Schepens A, Mullett HJ. A cadaveric model for suprascapular nerve injury during glenoid component screw insertion in reverse-geometry shoulder arthroplasty. J Shoulder Elbow Surg. 2011;20(8): 1323–7.
69. Nowak DD, Bahu MJ, Gardner TR, Dyrszka MD, Levine WN, Bigliani LU, et al. Simulation of surgical glenoid resurfacing using three-dimensional computed tomography of the arthritic glenohumeral joint: the amount of glenoid retroversion that can be

corrected. J Shoulder Elbow Surg. 2009;18(5): 680–8.
70. Nowak DD, Gardner TR, Bigliani LU, Levine WN, Ahmad CS. Interobserver and intraobserver reliability of the Walch classification in primary glenohumeral arthritis. J Shoulder Elbow Surg. 2010;19 (2):180–3.
71. Nuttall D, Haines JF, Trail II. A study of the micromovement of pegged and keeled glenoid components compared using radiostereometric analysis. J Shoulder Elbow Surg. 2007;16(3 Suppl):S65–70.
72. Nyffeler RW, Anglin C, Sheikh R, Gerber C. Influence of peg design and cement mantle thickness on pullout strength of glenoid component pegs. J Bone Joint Surg Br Vol. 2003;85(5):748–52.
73. Nyffeler RW, Jost B, Pfirrmann CWA, Gerber C. Measurement of glenoid version: conventional radiographs versus computed tomography scans. J Shoulder Elb Surg. 2003;12(5):493–6.
74. Nyffeler RW, Meyer D, Sheikh R, Koller BJ, Gerber C. The effect of cementing technique on structural fixation of pegged glenoid components in total shoulder arthroplasty. J Shoulder Elbow Surg. 2006; 15(1):106–11.
75. Nyffeler RW, Sheikh R, Atkinson TS, Jacob HA, Favre P, Gerber C. Effects of glenoid component version on humeral head displacement and joint reaction forces: an experimental study. J Shoulder Elbow Surg. 2006;15(5):625–9.
76. Orr TE, Carter DR, Schurman DJ. Stress analyses of glenoid component designs. Clin Orthop Relat Res. 1988;232:217–24.
77. Paisley KC, Kraeutler MJ, Lazarus MD, Ramsey ML, Williams GR, Smith MJ. Relationship of scapular neck length to scapular notching after reverse total shoulder arthroplasty by use of plain radiographs. J Shoulder Elbow Surg. 2014;23(6):882–7.
78. Papadonikolakis A, Matsen 3rd FA. Metal-backed glenoid components have a higher rate of failure and fail by different modes in comparison with all-polyethylene components: a systematic review. J Bone Joint Surg Am. 2014;96(12):1041–7.
79. Parsons BO, Gruson KI, Accousti KJ, Klug RA, Flatow EL. Optimal rotation and screw positioning for initial glenosphere baseplate fixation in reverse shoulder arthroplasty. J Shoulder Elbow Surg. 2009; 18(6):886–91.
80. Pilliar RM, Cameron HU, Macnab I. Porous surface layered prosthetic devices. Biomed Eng. 1975;10(4): 126–31.
81. Rahme H, Mattsson P, Wikblad L, Nowak J, Larsson S. Stability of cemented in-line pegged glenoid compared with keeled glenoid components in total shoulder arthroplasty. J Bone Joint Surg Am. 2009;91 (8):1965–72.
82. Roche CP, Stroud NJ, Martin BL, Steiler CA, Flurin PH, Wright TW, et al. The impact of scapular notching on reverse shoulder glenoid fixation. J Shoulder Elbow Surg. 2013;22(7):963–70.
83. Sabesan V, Callanan M, Ho J, Iannotti JP. Clinical and radiographic outcomes of total shoulder arthroplasty with bone graft for osteoarthritis with severe glenoid bone loss. J Bone Joint Surg Am. 2013; 95(14):1290–6.
84. Sabesan V, Callanan M, Sharma V, Iannotti JP. Correction of acquired glenoid bone loss in osteoarthritis with a standard versus an augmented glenoid component. J Shoulder Elbow Surg. 2014;23 (7):964–73.
85. Sabesan VJ, Ackerman J, Sharma V, Baker KC, Kurdziel MD, Wiater JM. Glenohumeral mismatch affects micromotion of cemented glenoid components in total shoulder arthroplasty. J Shoulder Elbow Surg. 2015;24(5):814–22.
86. Scalise JJ, Codsi MJ, Brems JJ, Iannotti JP. Interrater reliability of an arthritic glenoid morphology classification system. J Shoulder Elbow Surg. 2008;17(4):575–7.
87. Scalise JJ, Codsi MJ, Bryan J, Iannotti JP. The three-dimensional glenoid vault model can estimate normal glenoid version in osteoarthritis. J Shoulder Elbow Surg. 2008;17(3):487–91.
88. Simovitch RW, Zumstein MA, Lohri E, Helmy N, Gerber C. Predictors of scapular notching in patients managed with the Delta III reverse total shoulder replacement. J Bone Joint Surg Am. 2007;89(3): 588–600.
89. Smith SP, Bunker TD. Primary glenoid dysplasia. A review of 12 patients. J Bone Joint Surg Br Vol. 2001;83(6):868–72.
90. Stephens BF, Hebert CT, Azar FM, Mihalko WM, Throckmorton TW. Optimal baseplate rotational alignment for locking-screw fixation in reverse total shoulder arthroplasty: a three-dimensional computer-aided design study. J Shoulder Elbow Surg. 2015; 24(9):1367–71.
91. Stephens SP, Paisley KC, Jeng J, Dutta AK, Wirth MA. Shoulder arthroplasty in the presence of posterior glenoid bone loss. J Bone Joint Surg Am. 2015;97(3):251–9.
92. Stone KD, Grabowski JJ, Cofield RH, Morrey BF, An KN. Stress analyses of glenoid components in total shoulder arthroplasty. J Shoulder Elbow Surg. 1999;8(2):151–8.
93. Torrens C, Corrales M, Gonzalez G, Solano A, Caceres E. Cadaveric and three-dimensional computed tomography study of the morphology of the scapula with reference to reversed shoulder prosthesis. J Orthop Surg Res. 2008;3:49.
94. Vavken P, Sadoghi P, von Keudell A, Rosso C, Valderrabano V, Muller AM. Rates of radiolucency and loosening after total shoulder arthroplasty with pegged or keeled glenoid components. J Bone Joint Surg Am. 2013;95(3):215–21.
95. Visotsky JL, Basamania C, Seebauer L, Rockwood CA, Jensen KL. Cuff tear arthropathy: pathogenesis, classification, and algorithm for treatment. J Bone Joint Surg Am. 2004;86-A Suppl 2:35–40.

96. Walch G, Badet R, Boulahia A, Khoury A. Morphologic study of the glenoid in primary glenohumeral osteoarthritis. J Arthroplast. 1999;14 (6):756–60.
97. Walch G, Edwards TB, Boulahia A, Boileau P, Mole D, Adeleine P. The influence of glenohumeral prosthetic mismatch on glenoid radiolucent lines: results of a multicenter study. J Bone Joint Surg Am. 2002; 84-a(12):2186–91.
98. Wang J, Singh A, Higgins L, Warner J. Suprascapular neuropathy secondary to reverse shoulder arthroplasty: a case report. J Shoulder Elbow Surg. 2010; 19(3):e5–8.
99. Wang T, Abrams GD, Behn AW, Lindsey D, Giori N, Cheung EV. Posterior glenoid wear in total shoulder arthroplasty: eccentric anterior reaming is superior to posterior augment. Clin Orthop Relat Res. 2015; 473:3928–36.
100. Wirth MA, Klotz C, Deffenbaugh DL, McNulty D, Richards L, Tipper JL. Cross-linked glenoid prosthesis: a wear comparison to conventional glenoid prosthesis with wear particulate analysis. J Shoulder Elbow Surg. 2009;18(1):130–7.
101. Wirth MA, Korvick DL, Basamania CJ, Toro F, Aufdemorte TB, Rockwood Jr CA. Radiologic, mechanical, and histologic evaluation of 2 glenoid prosthesis designs in a canine model. J Shoulder Elbow Surg. 2001;10(2):140–8.
102. Yian EH, Werner CM, Nyffeler RW, Pfirrmann CW, Ramappa A, Sukthankar A, et al. Radiographic and computed tomography analysis of cemented pegged polyethylene glenoid components in total shoulder replacement. J Bone Joint Surg Am. 2005;87(9):1928–36.
103. Yongpravat C, Kim HM, Gardner TR, Bigliani LU, Levine WN, Ahmad CS. Glenoid implant orientation and cement failure in total shoulder arthroplasty: a finite element analysis. J Shoulder Elbow Surg. 2013;22(7):940–7.